



The  
University  
Of  
Sheffield.

THE  
ROYAL  
SOCIETY

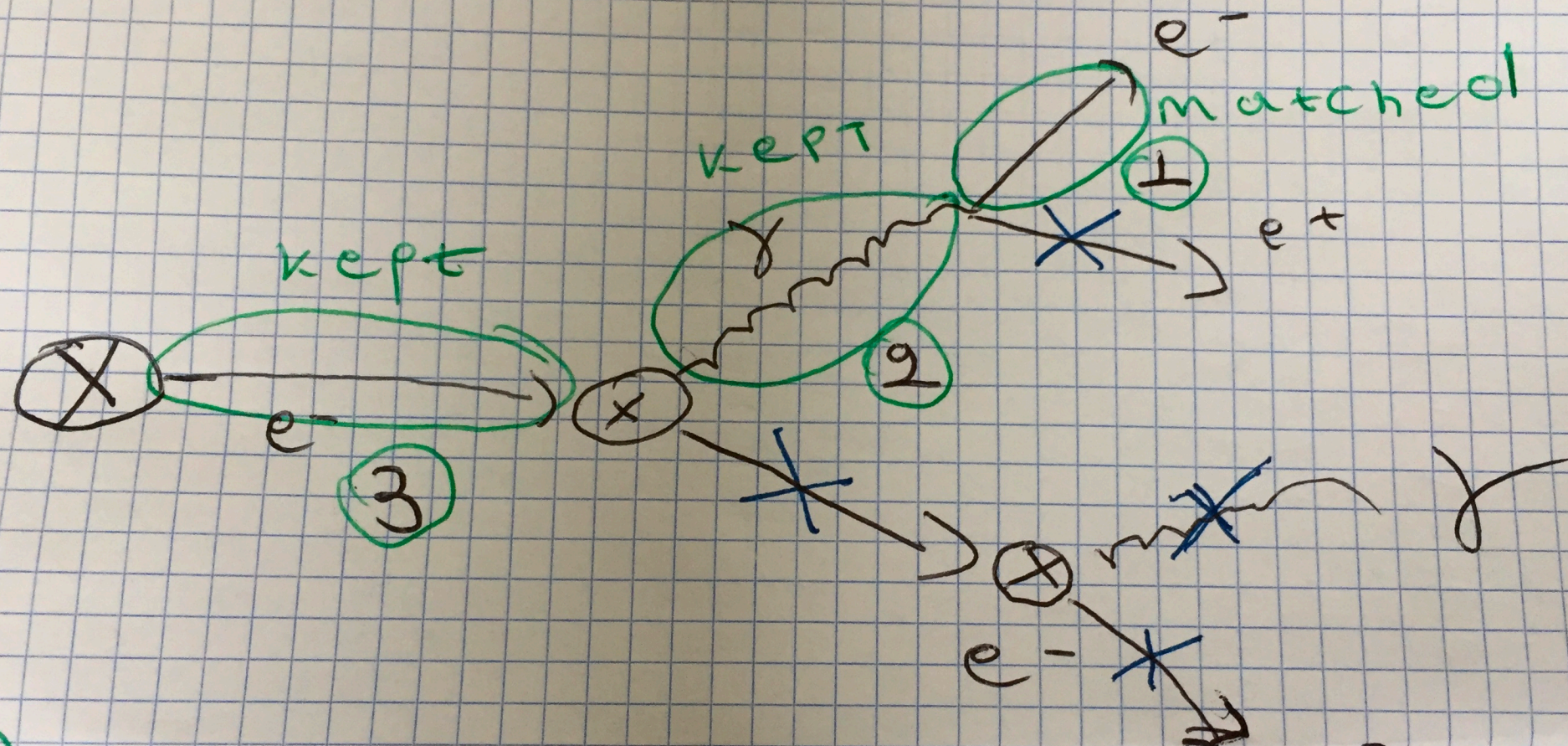
$e/\gamma$

Reconstruction in ATLAS  
Christos Anastopoulos

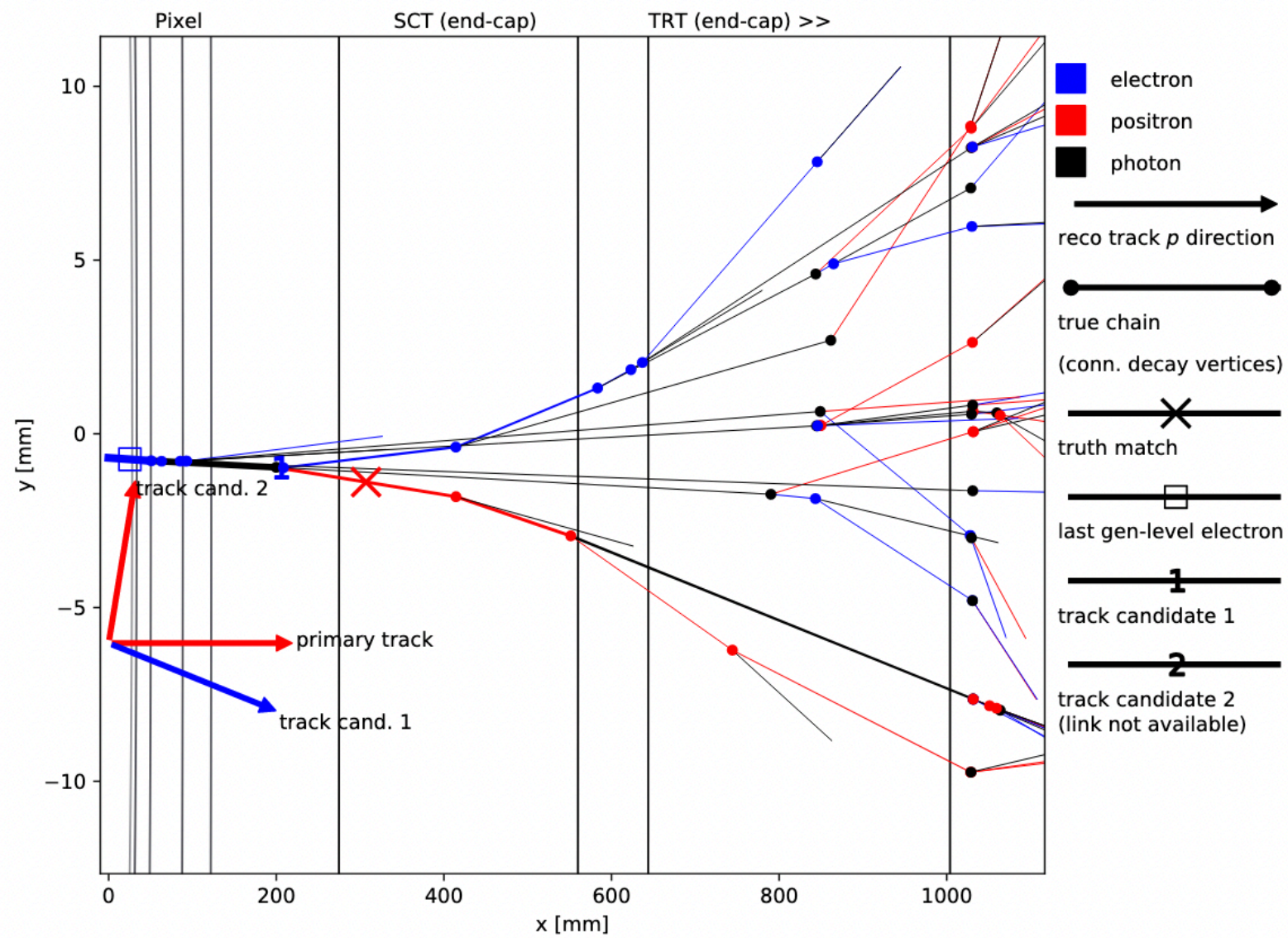




# AOD T20TH SLIM







variable	last gen-ele.	truth link	reco ele.	primary track
$p_T$ [GeV] :	49.5496	20.3452	48.7104	101.229
$\eta$ :	-1.91653	-1.91653	-1.91673	-1.91673
$\phi$ :	-0.573253	-0.572522	-0.571249	-0.571249
$\Delta R$ to reco ele :	0.002	0.001	0.000	0.000
PDG ID / charge :	11	-11	1	1
barcode :	10001	200015	---	---
BL hits :	---	---	---	1
PIX hits :	---	---	---	4
SCT hits :	---	---	---	12
innermost PIX :	---	---	---	1
next-to-inn. PIX :	---	---	---	1
match probability :	---	---	---	0.674797

# e/ $\gamma$ reconstruction

## Relevant Publications

Broadly e/ $\gamma$  at “core” reconstruction level deals with calorimeter clusters and inner detector tracks to define :

- Electrons
- Converted Photon
- Unconverted Photons

In a later stages e/ $\gamma$  deals with :

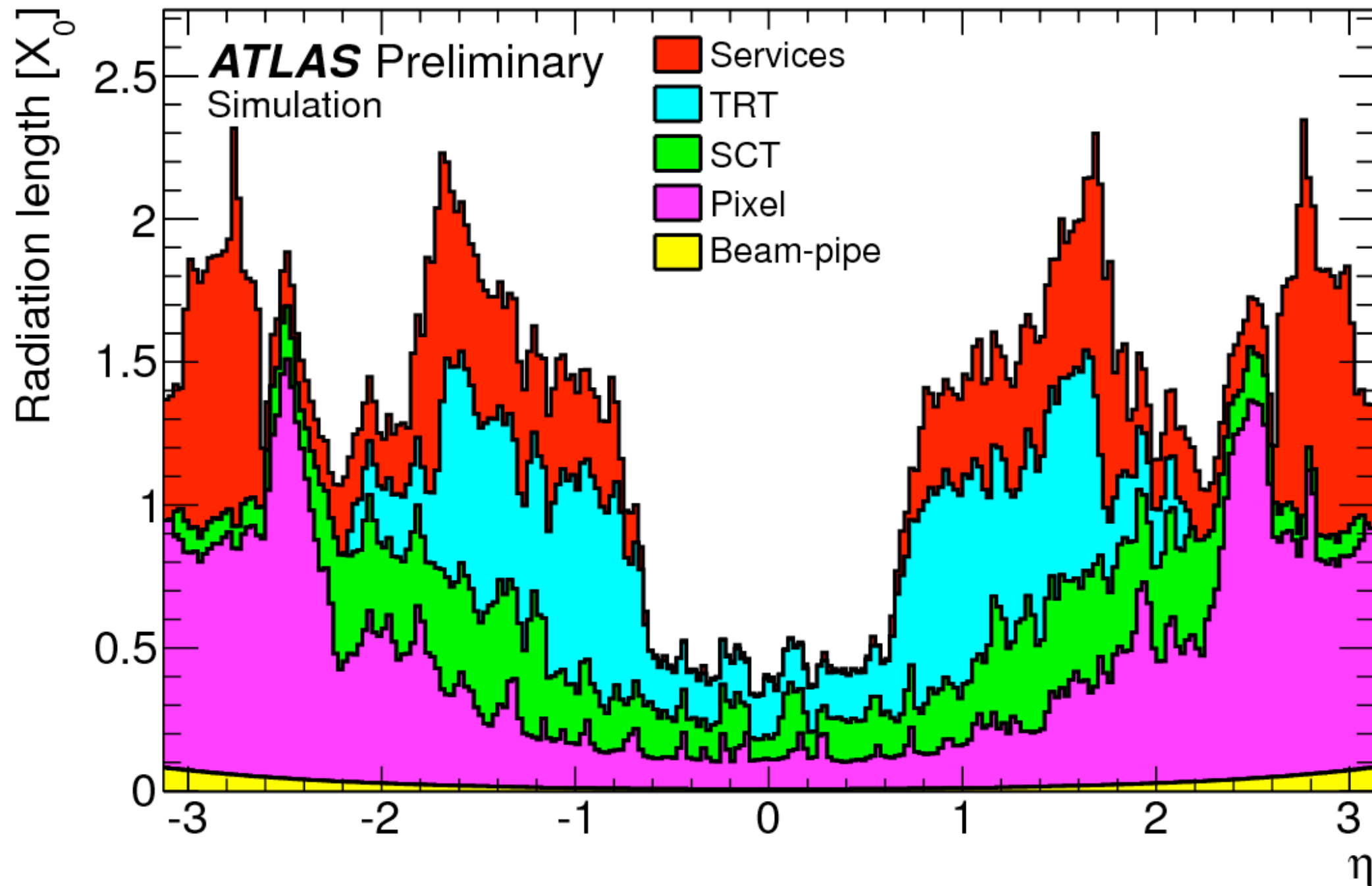
- Electron / photon energy calibrations
- Electron Identification
- Photon Identification

At a more “analysis” level derive the relevant data/MC corrections



# e/ $\gamma$ reconstruction

The main challenge is that electron/photons can and will “brem”/ “convert” in the presence of material.



# e/ $\gamma$ reconstruction

The main challenge is that electron/photons will “brem”/ “convert” in the presence of material.

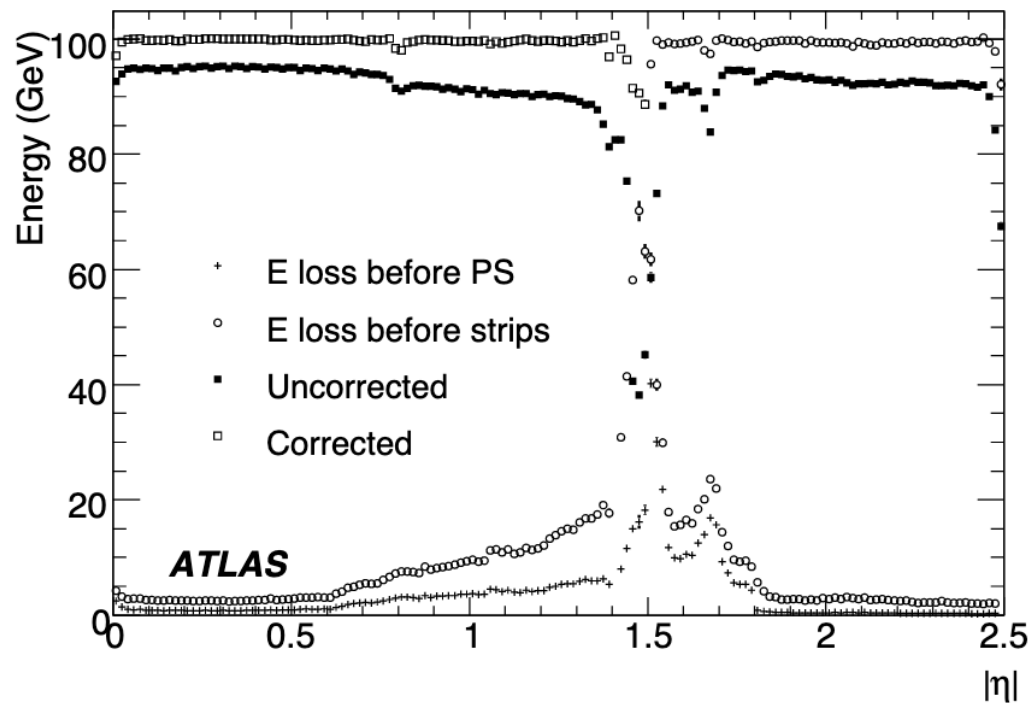


Figure 1: Average energy loss vs.  $|\eta|$  for  $E = 100$  GeV electrons before the presampler/strips (crosses/open circles), and reconstructed energies before/after (solid/open boxes) corrections.

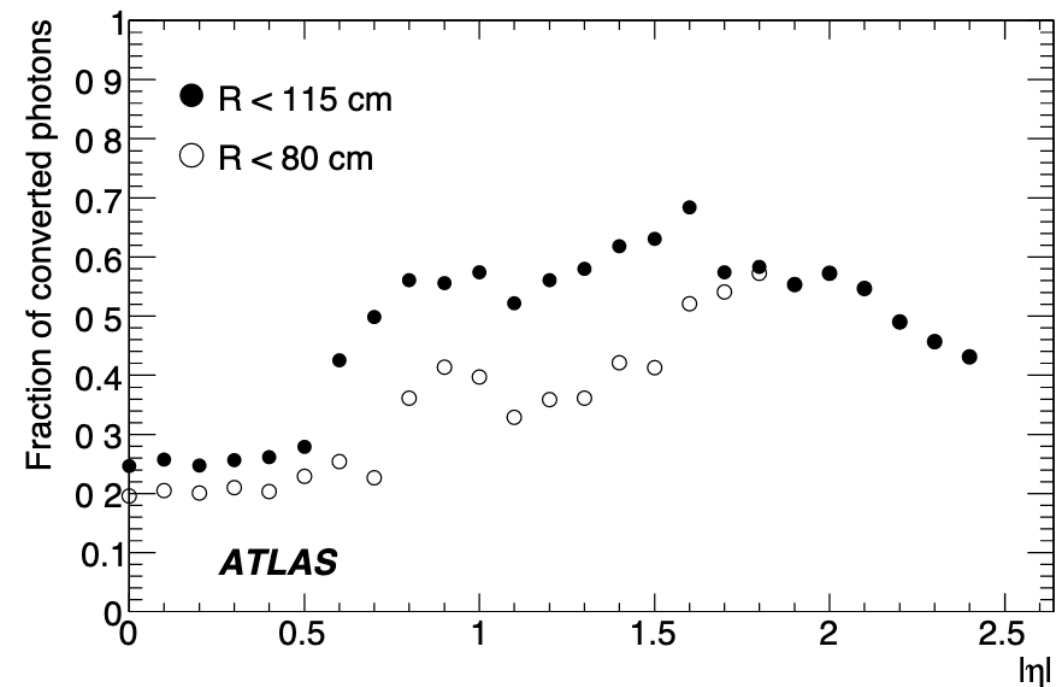
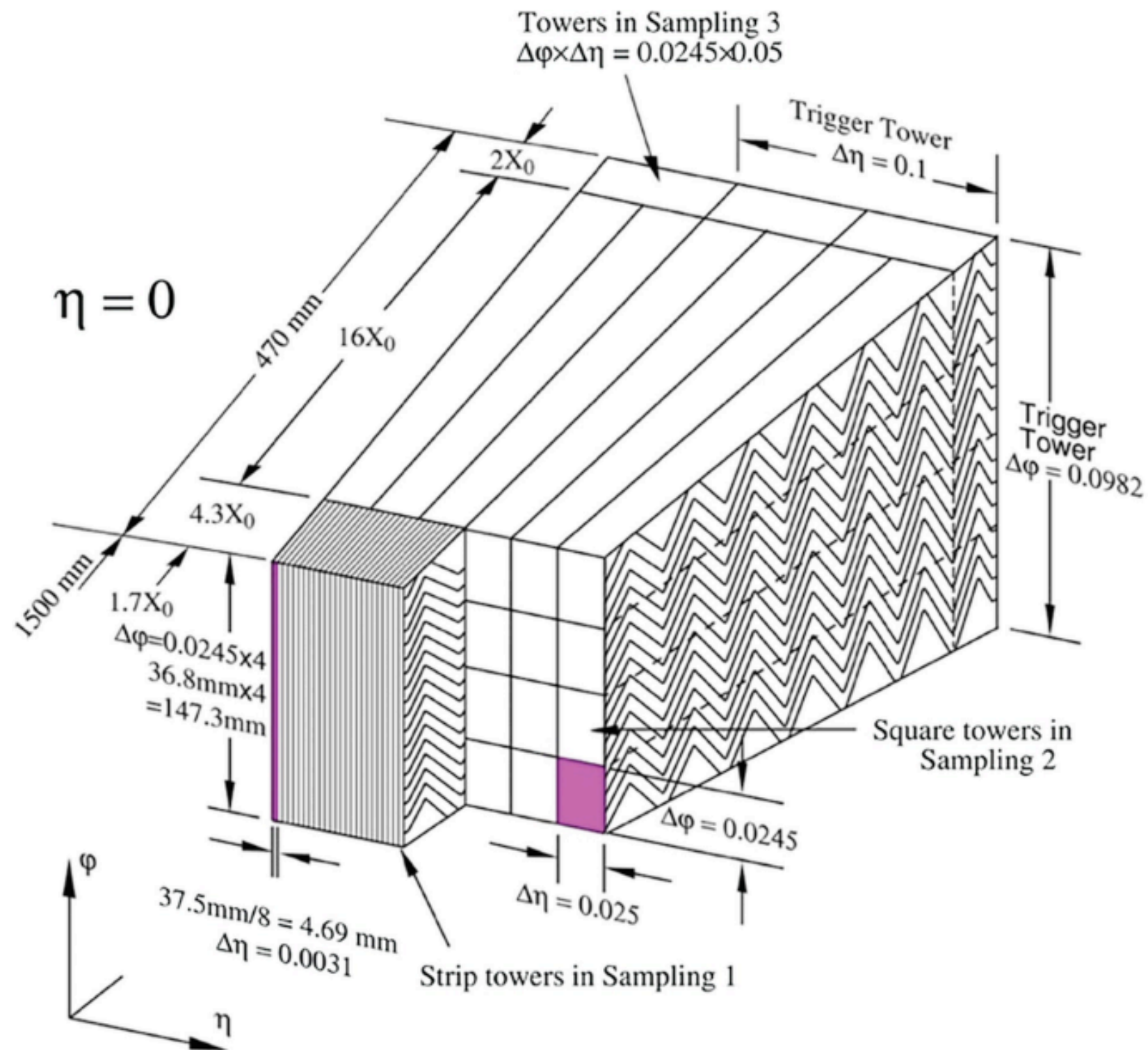


Figure 2: Fraction of photons converting at a radius of below 80 cm (115 cm) in open (full) circles, as a function of  $|\eta|$  [4].



# e/γ Calorimeter Clusters

Important note the usual unit of size is a cells in the middle sampling (0.025x0.025)



# e/γ Calorimeter Clusters

For a calorimeter like the ATLAS EM one needs to keep the size relatively small.  
During test beam size a 3x3 size was used for electrons

During Run-I different sizes for electrons/conversions vs unconverted were already into place e.g see

The effect of the choice of cluster size on electron and photon energy reconstruction has been studied in Refs. [1] and [8]. These results are still the baseline of the present software. For electrons, the energy in the barrel electromagnetic calorimeter is collected over an area corresponding to  $3 \times 7$  cells in the middle layer, i.e.  $\Delta\eta \times \Delta\phi = 0.075 \times 0.175$ . For unconverted photons, the area is limited to  $3 \times 5$  cells in the middle layer, whereas converted photons are treated like electrons. The cluster width in  $\eta$  increases

These are usually called “fixed-size” clusters.

In the past were “seeded” by a so called sliding-window algorithm.  
But could be also be seeded on top of topological clusters.



# e/γ Calorimeter Clusters

## Topological cluster in ATLAS

$$\varsigma_{\text{cell}}^{\text{EM}} = \frac{E_{\text{cell}}^{\text{EM}}}{\sigma_{\text{noise,cell}}^{\text{EM}}}. \quad (2)$$

Both the cell signal  $E_{\text{cell}}^{\text{EM}}$  and  $\sigma_{\text{noise,cell}}^{\text{EM}}$  are measured on the electromagnetic (EM) energy scale. This scale reconstructs the energy deposited by electrons and photons correctly but does not include any corrections for the loss of signal for hadrons due to the non-compensating character of the ATLAS calorimeters.

Topo-clusters are formed by a growing-volume algorithm starting from a calorimeter cell with a highly significant seed signal. The seeding, growth, and boundary features of topo-clusters are in this algorithm controlled by the three respective parameters  $\{S, N, P\}$ , which define signal thresholds in terms of  $\sigma_{\text{noise,cell}}^{\text{EM}}$  and thus apply selections based on  $\varsigma_{\text{cell}}^{\text{EM}}$  from Eq. (2),

$$|E_{\text{cell}}^{\text{EM}}| > S \sigma_{\text{noise,cell}}^{\text{EM}} \Rightarrow |\varsigma_{\text{cell}}^{\text{EM}}| > S \quad (\text{primary seed threshold, default } S = 4); \quad (3)$$

$$|E_{\text{cell}}^{\text{EM}}| > N \sigma_{\text{noise,cell}}^{\text{EM}} \Rightarrow |\varsigma_{\text{cell}}^{\text{EM}}| > N \quad (\text{threshold for growth control, default } N = 2); \quad (4)$$

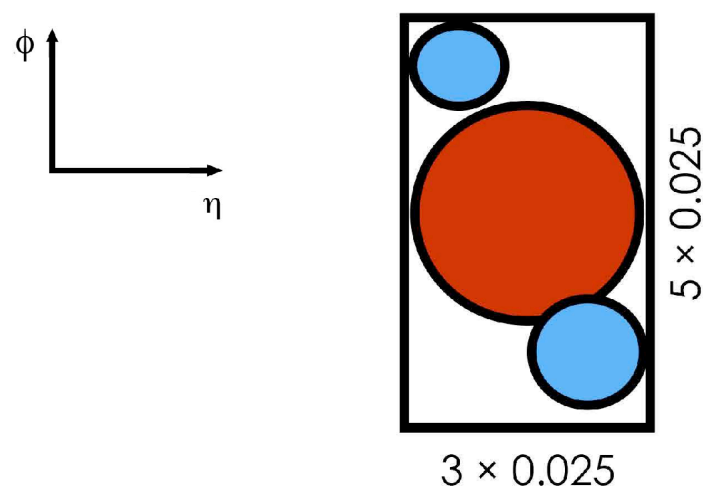
$$|E_{\text{cell}}^{\text{EM}}| > P \sigma_{\text{noise,cell}}^{\text{EM}} \Rightarrow |\varsigma_{\text{cell}}^{\text{EM}}| > P \quad (\text{principal cell filter, default } P = 0). \quad (5)$$

# e/ $\gamma$ Calorimeter Clusters

Start from topological clusters “close” together and pick their cells to create an e/ $\gamma$  cluster.

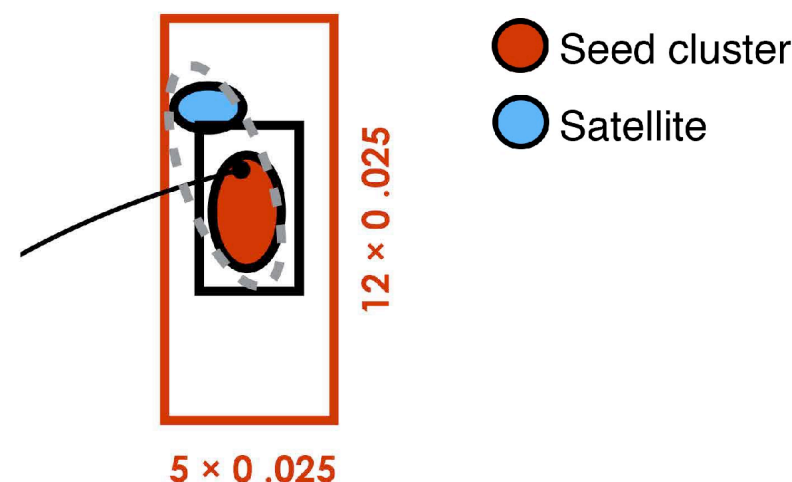
## All $e^\pm$ , $\gamma$ :

Add all clusters within  $3 \times 5$  window around seed cluster.



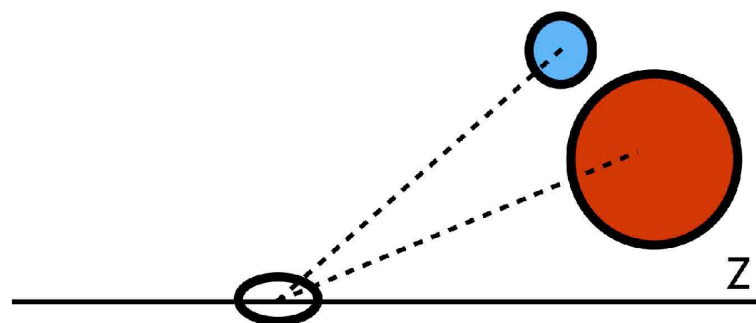
## Electrons only:

Seed, secondary cluster **match the same track**.

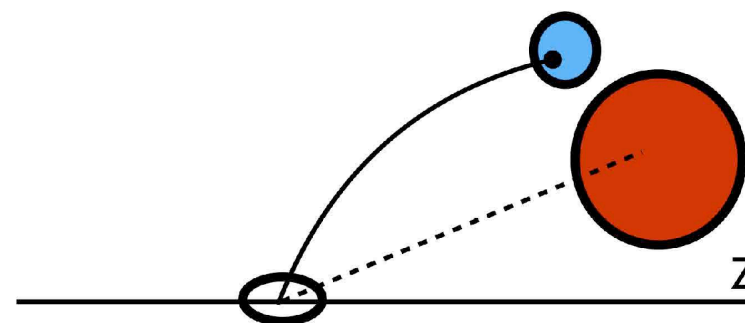


## Converted photons only:

Add topo-clusters that have the **same conversion vertex** matched as the seed cluster.



Add topo-clusters with a **track match** that is **part of the conversion vertex** matched to the seed cluster.

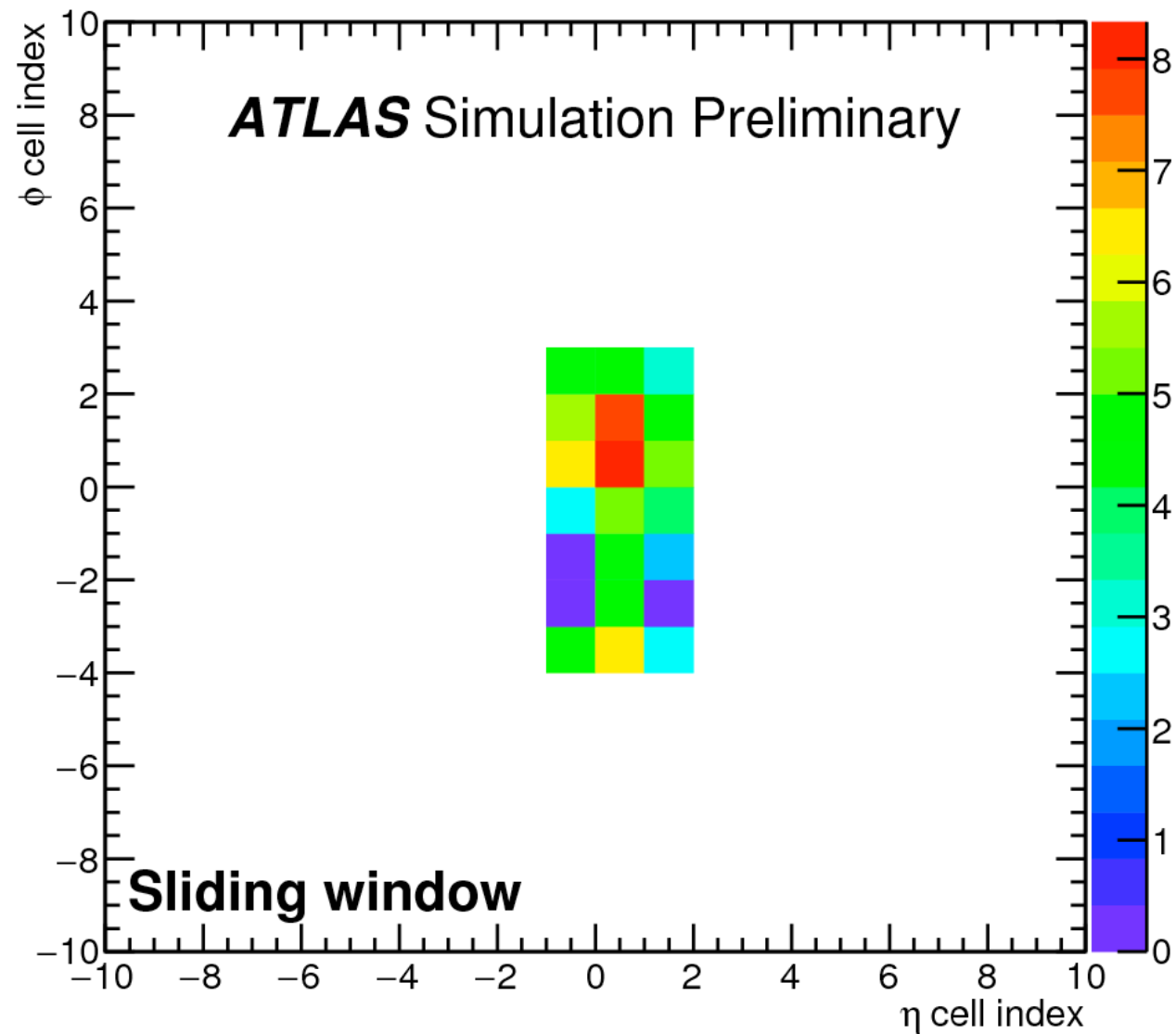




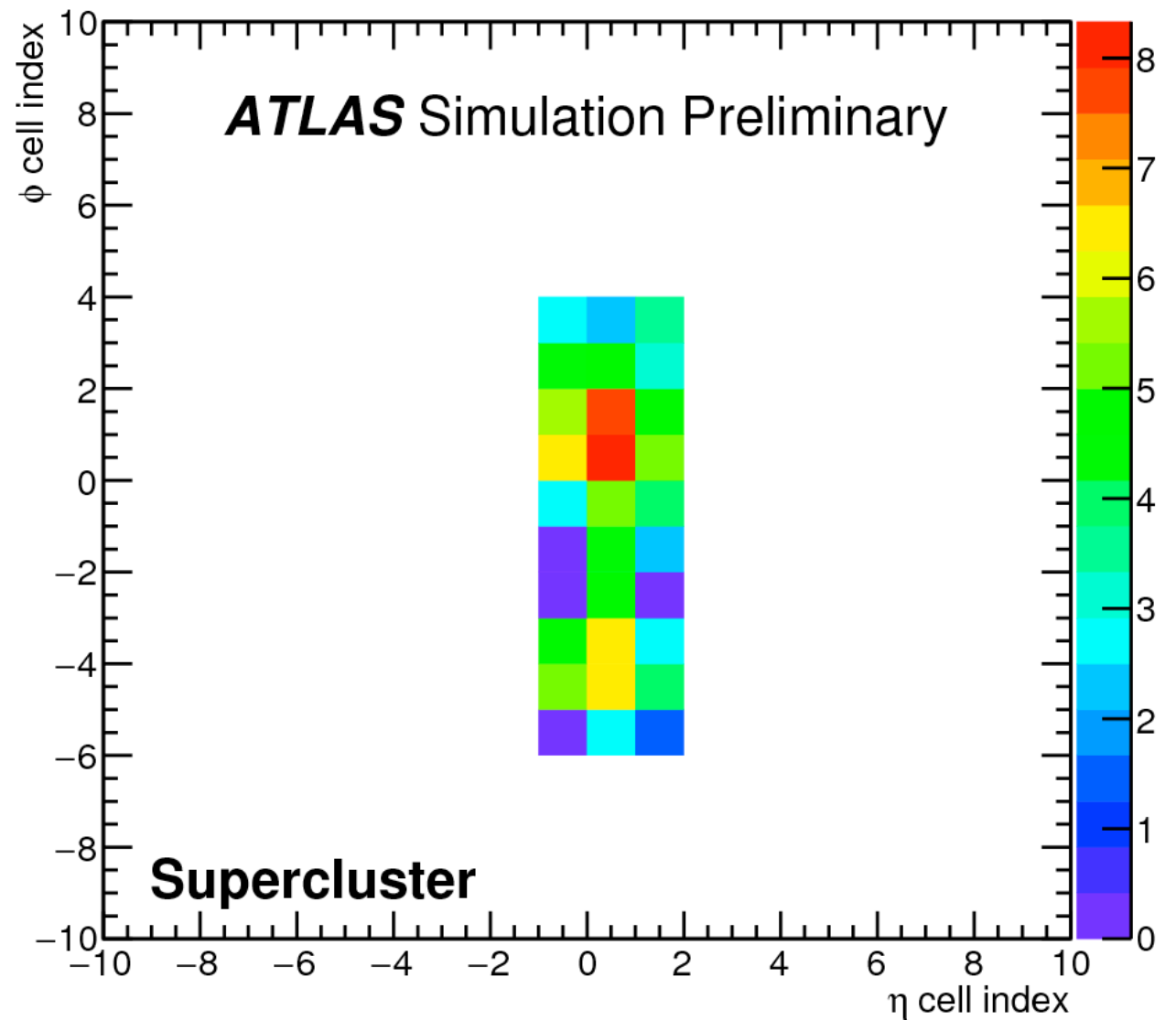
# e/γ Calorimeter Clusters

Start from topological clusters “close” together and pick their cells to create an e/γ cluster.

$E_{\text{Raw}} = 13.57 \text{ GeV}$ ,  $E_{\text{Gen}} = 17.59 \text{ GeV}$ ,  $\eta_{\text{Gen}} = -0.50$



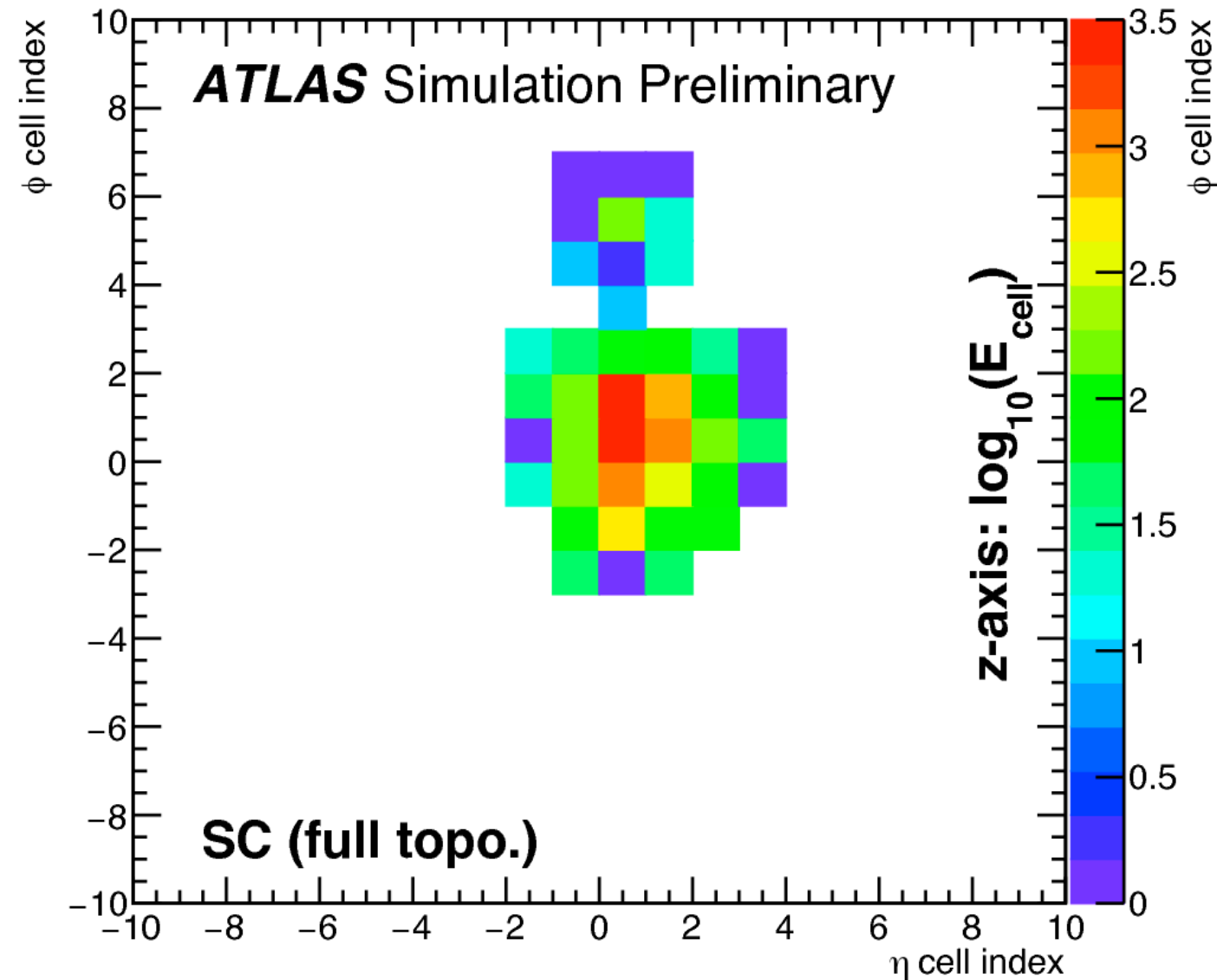
$E_{\text{Raw}} = 16.98 \text{ GeV}$ ,  $E_{\text{Gen}} = 17.59 \text{ GeV}$ ,  $\eta_{\text{Gen}} = -0.50$



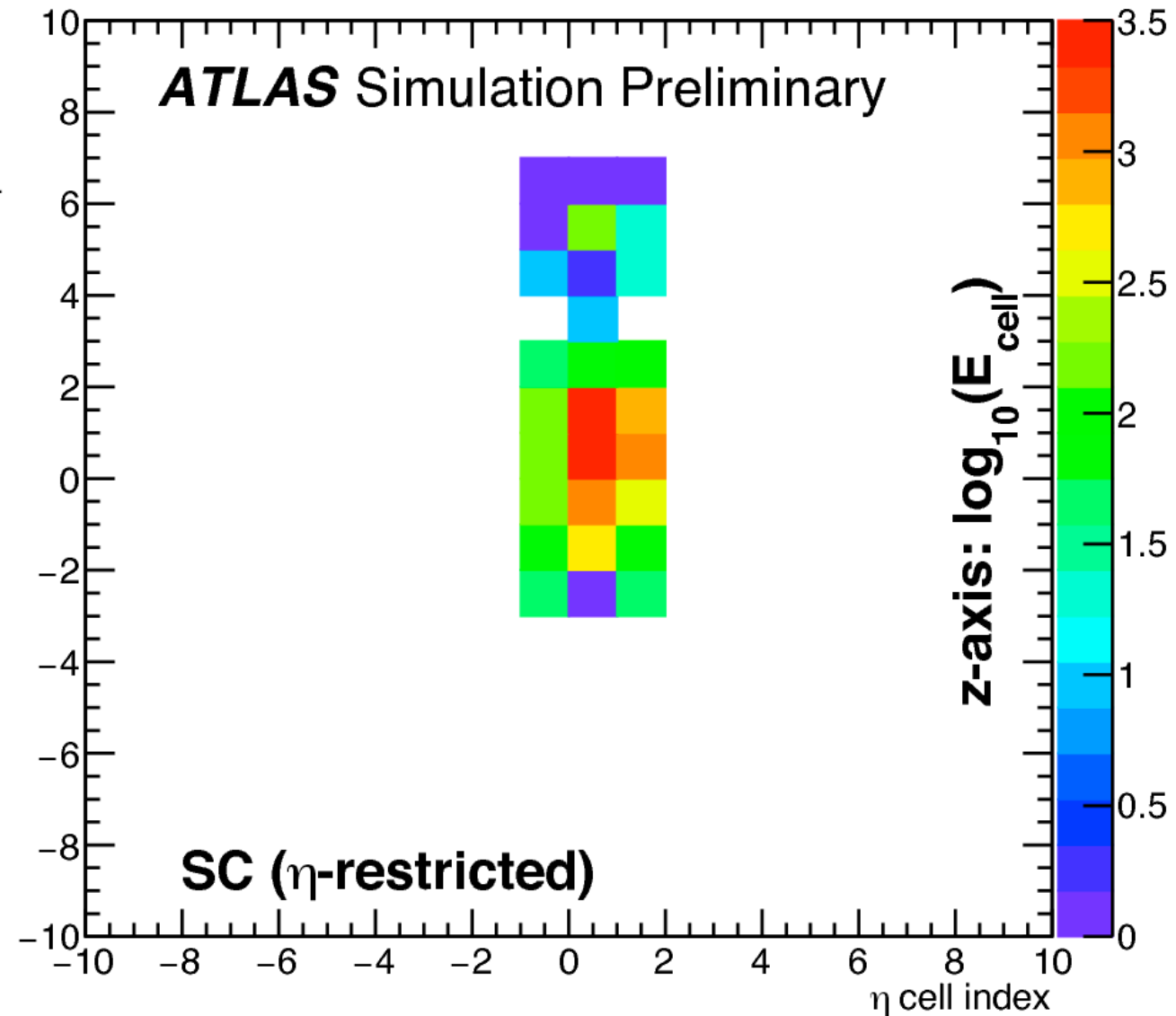
# e/ $\gamma$ Calorimeter Clusters

During Run-II ATLAS moved to “dynamic” clusters in  $\phi$  based on topological clusters

$E_{\text{raw}} = 16.19 \text{ GeV}$ ,  $E_{\text{true}} = 18.04 \text{ GeV}$ ,  $\eta_{\text{true}} = -1.02$



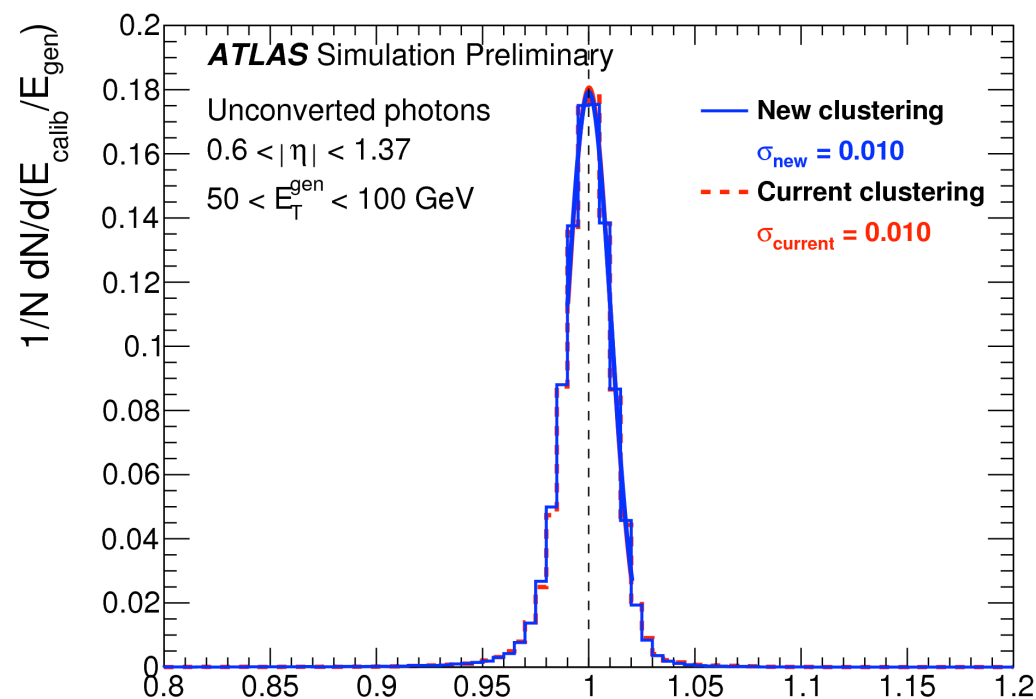
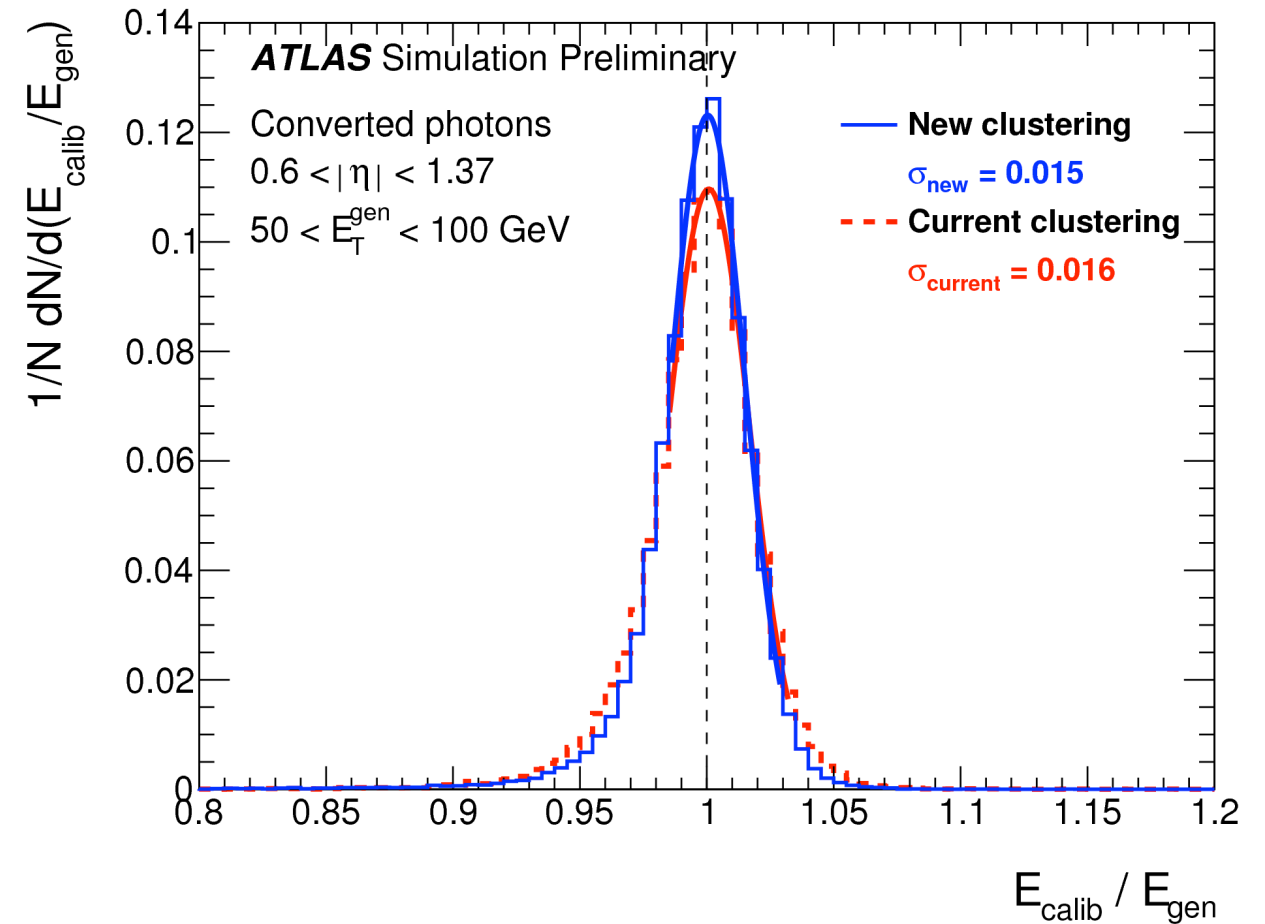
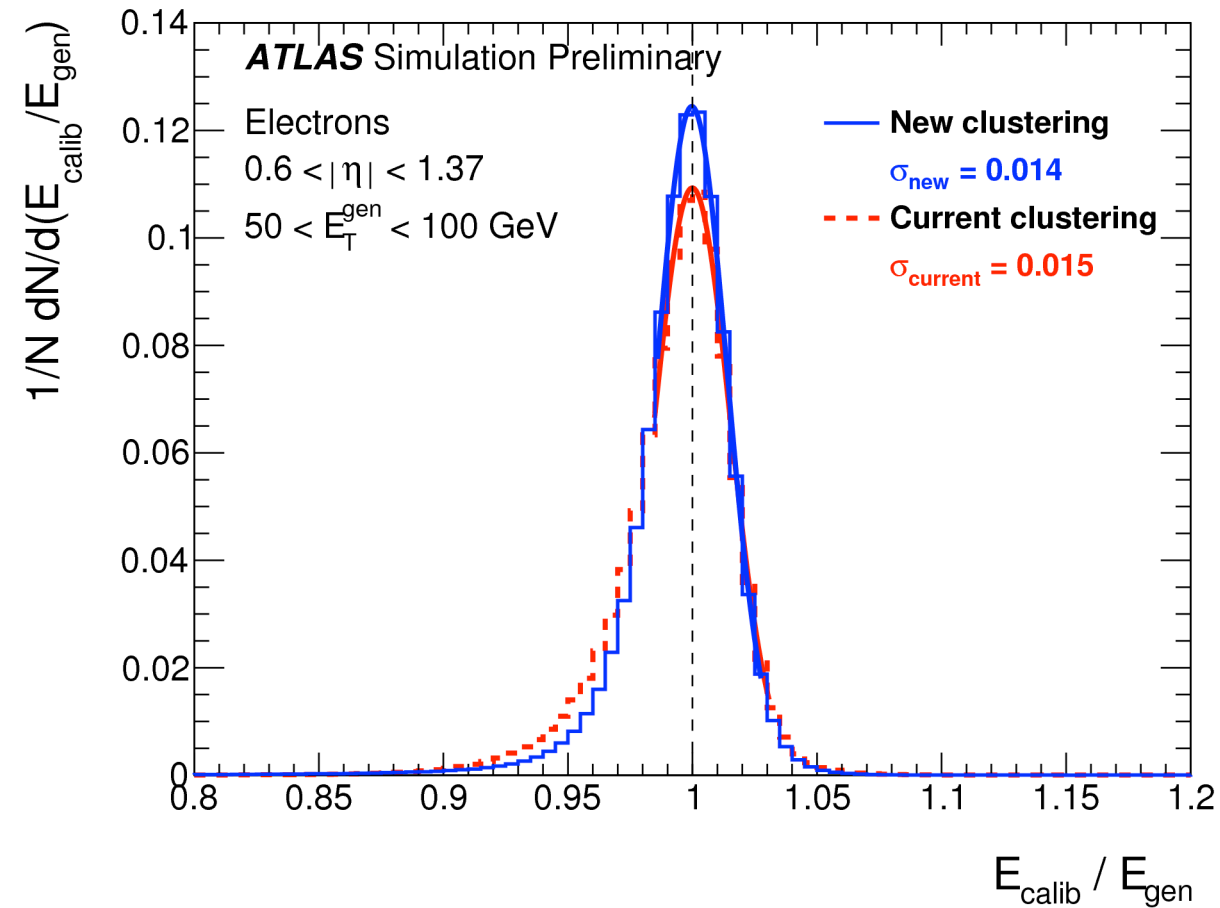
$E_{\text{raw}} = 15.62 \text{ GeV}$ ,  $E_{\text{true}} = 18.04 \text{ GeV}$ ,  $\eta_{\text{true}} = -1.02$





# e/γ Calorimeter Clusters

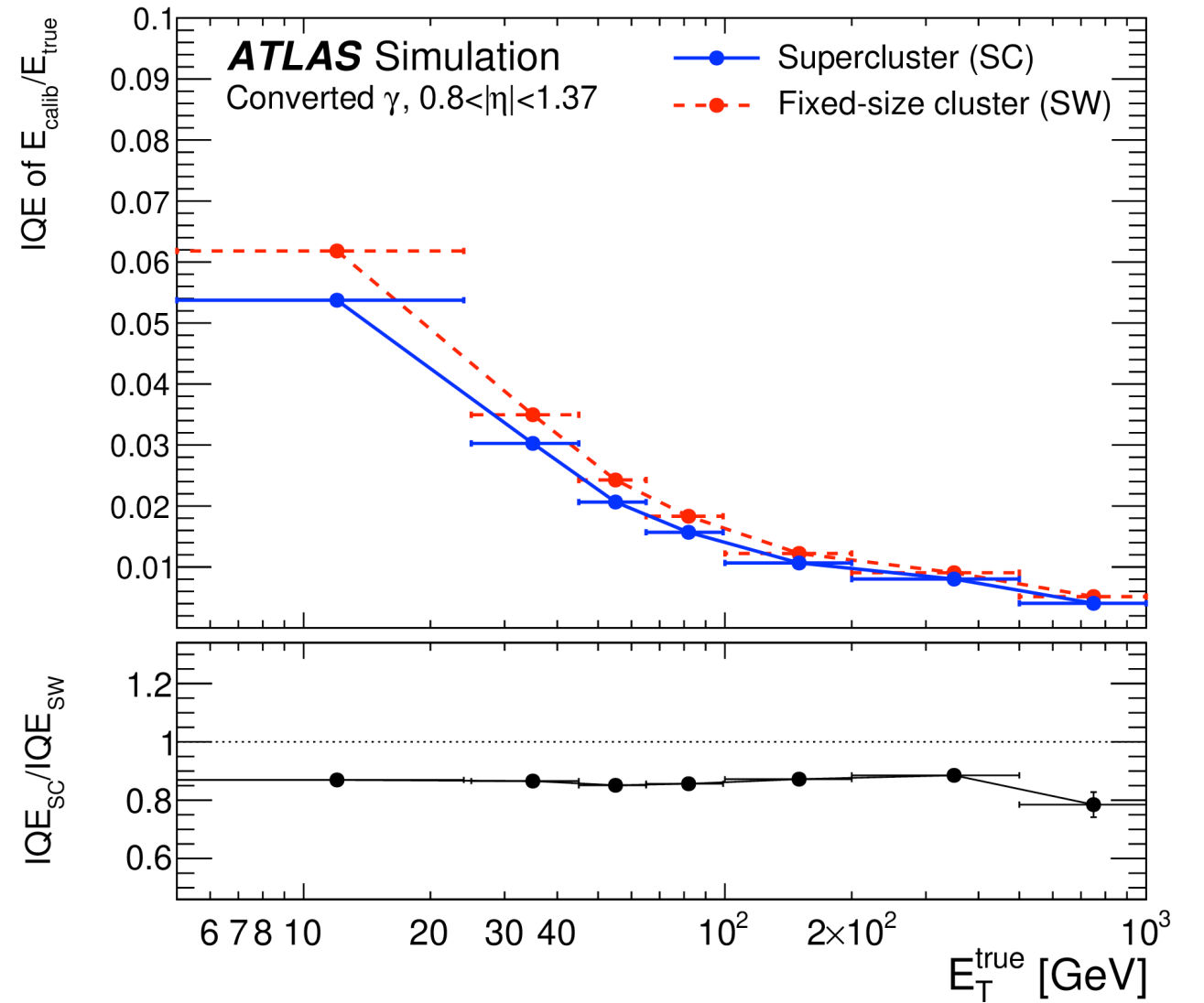
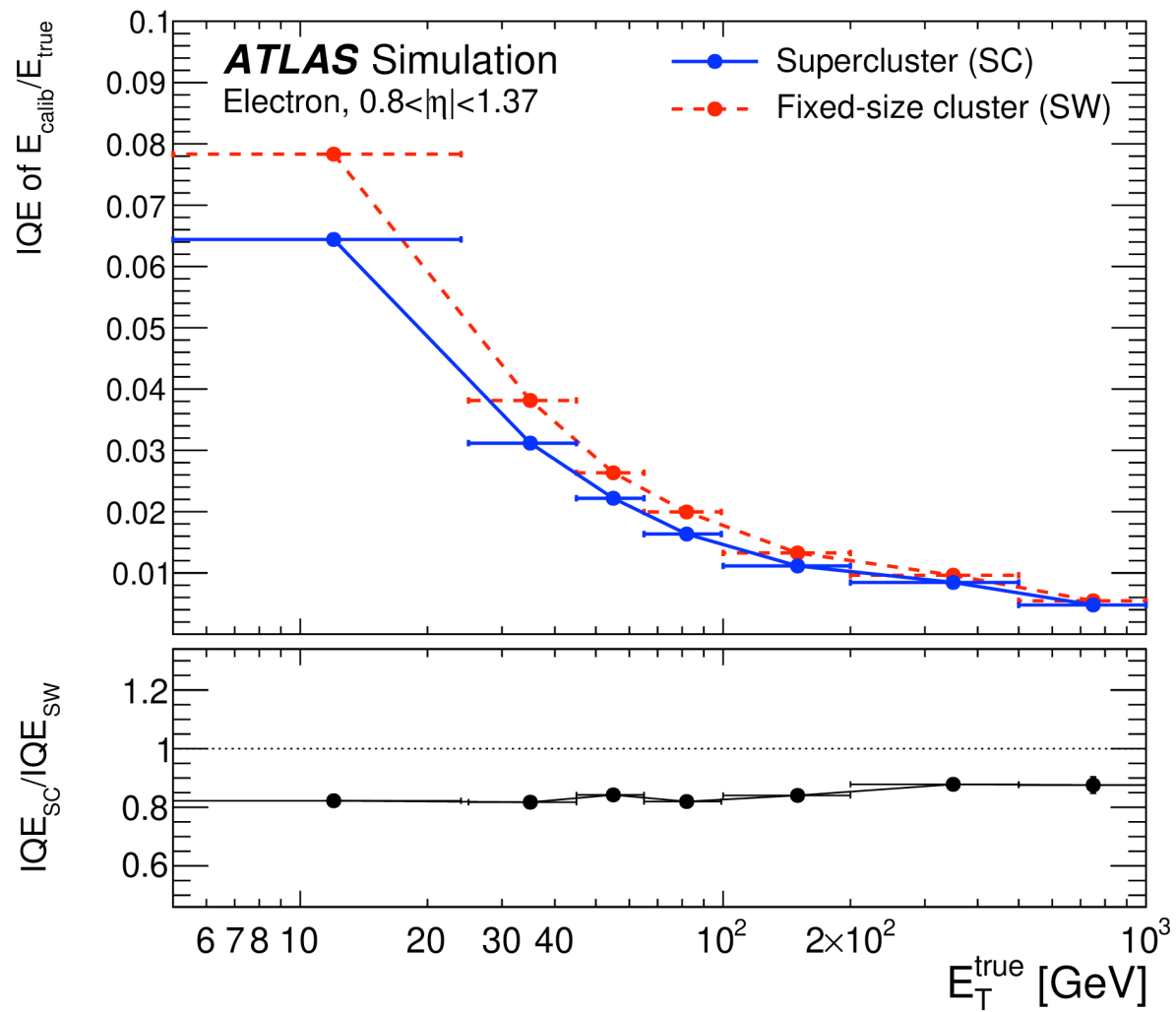
During Run-II ATLAS moved to “dynamic” clusters in  $\phi$  based on topological clusters



No difference for unconverted. Better for converted photons and electrons.

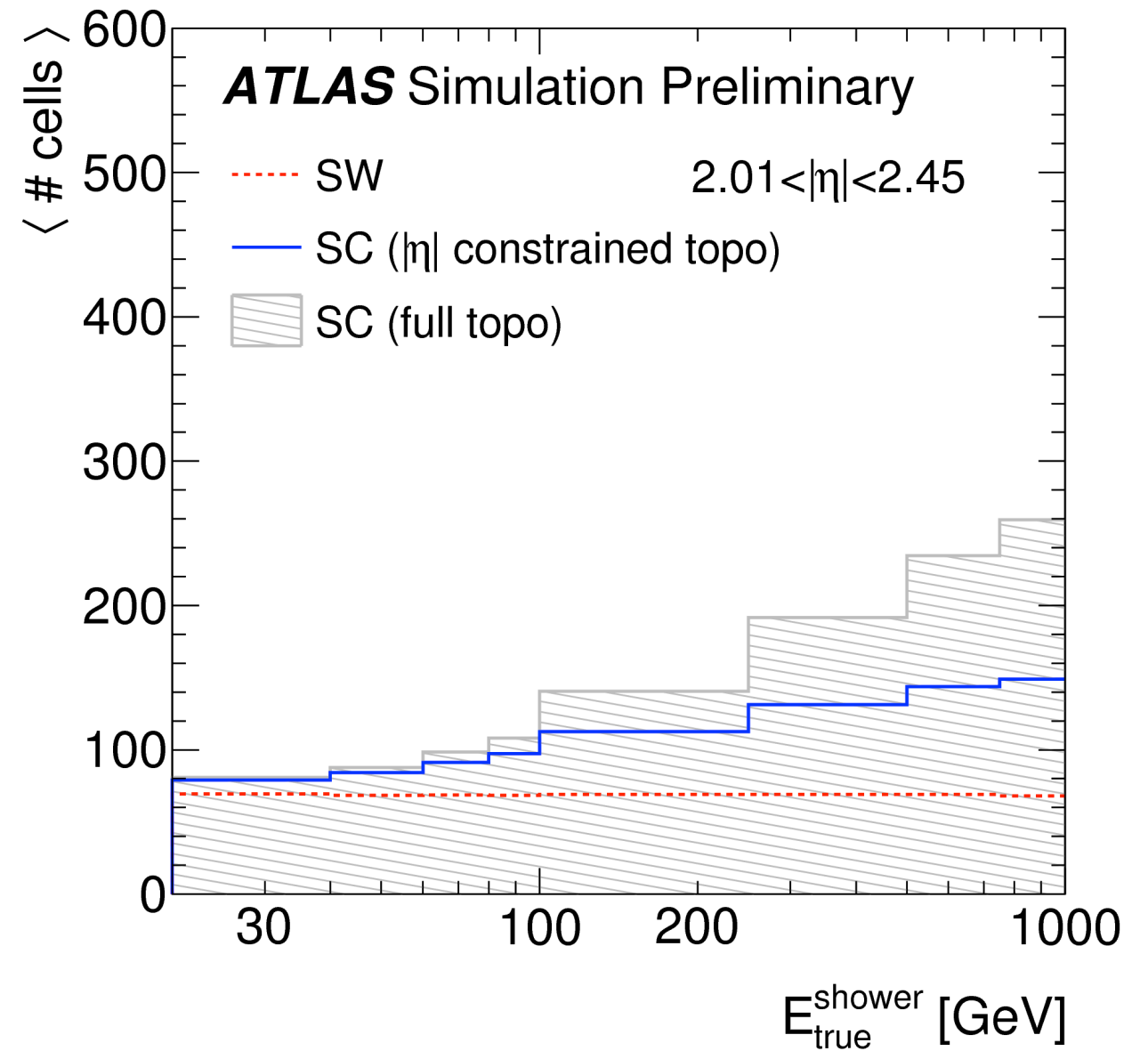
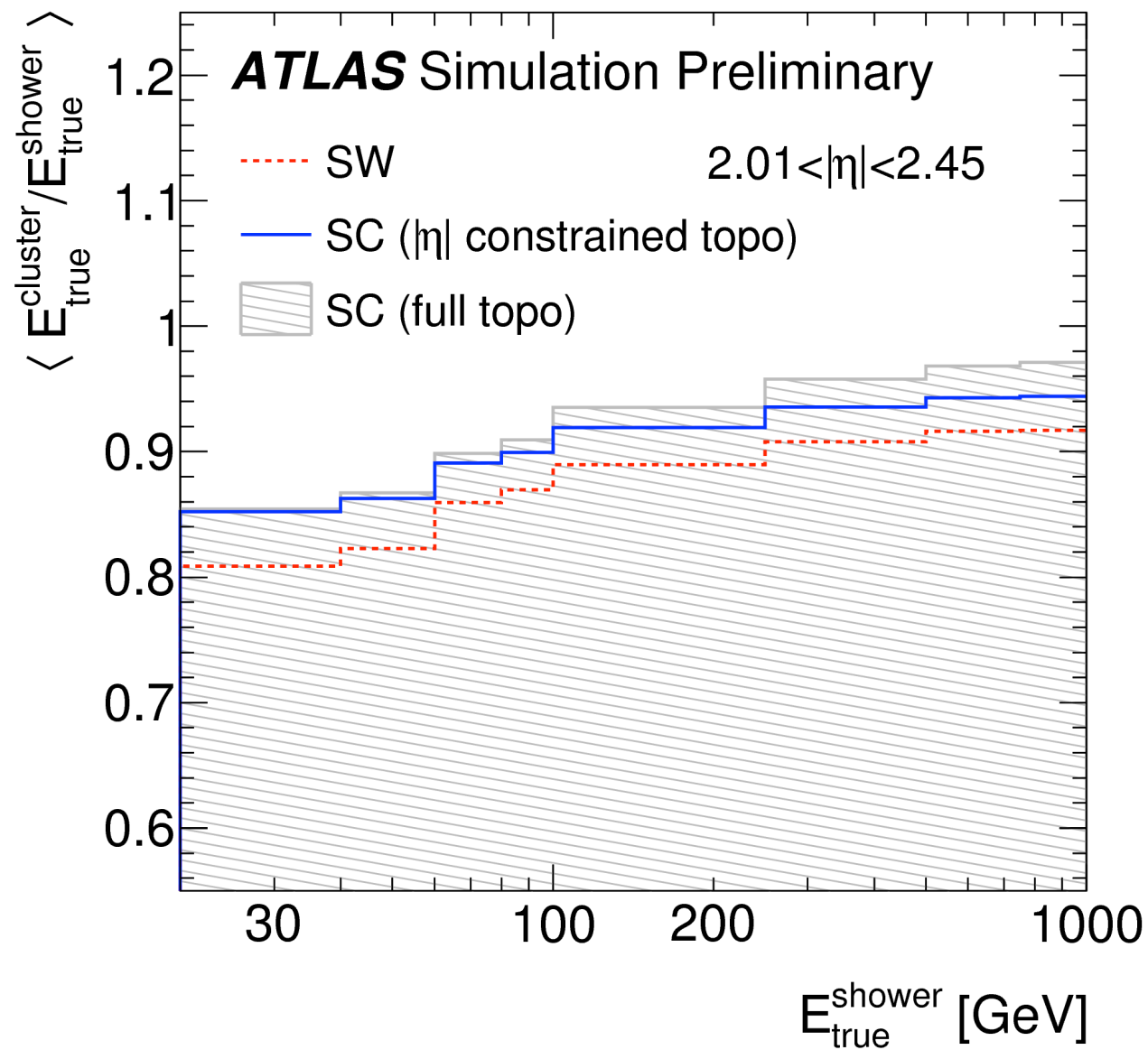
# e/γ Calorimeter Clusters

During Run-II ATLAS moved to “dynamic” clusters in  $\phi$  based on topological clusters



# e/γ Calorimeter Clusters

During Run-II ATLAS moved to “dynamic” clusters in  $\phi$  based on topological clusters



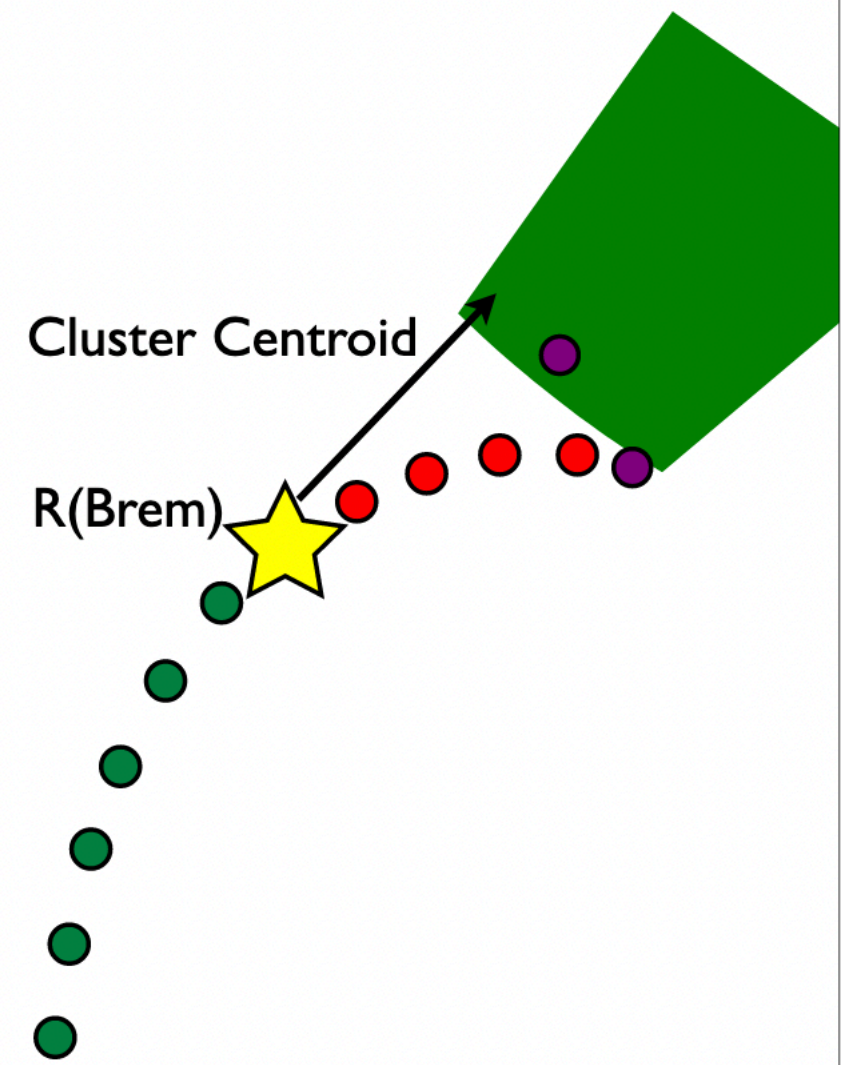


# An aside on the $\phi$ of the cluster

The cluster  $\phi \sim$  close to where the truth particle would have hit the calorimeter.

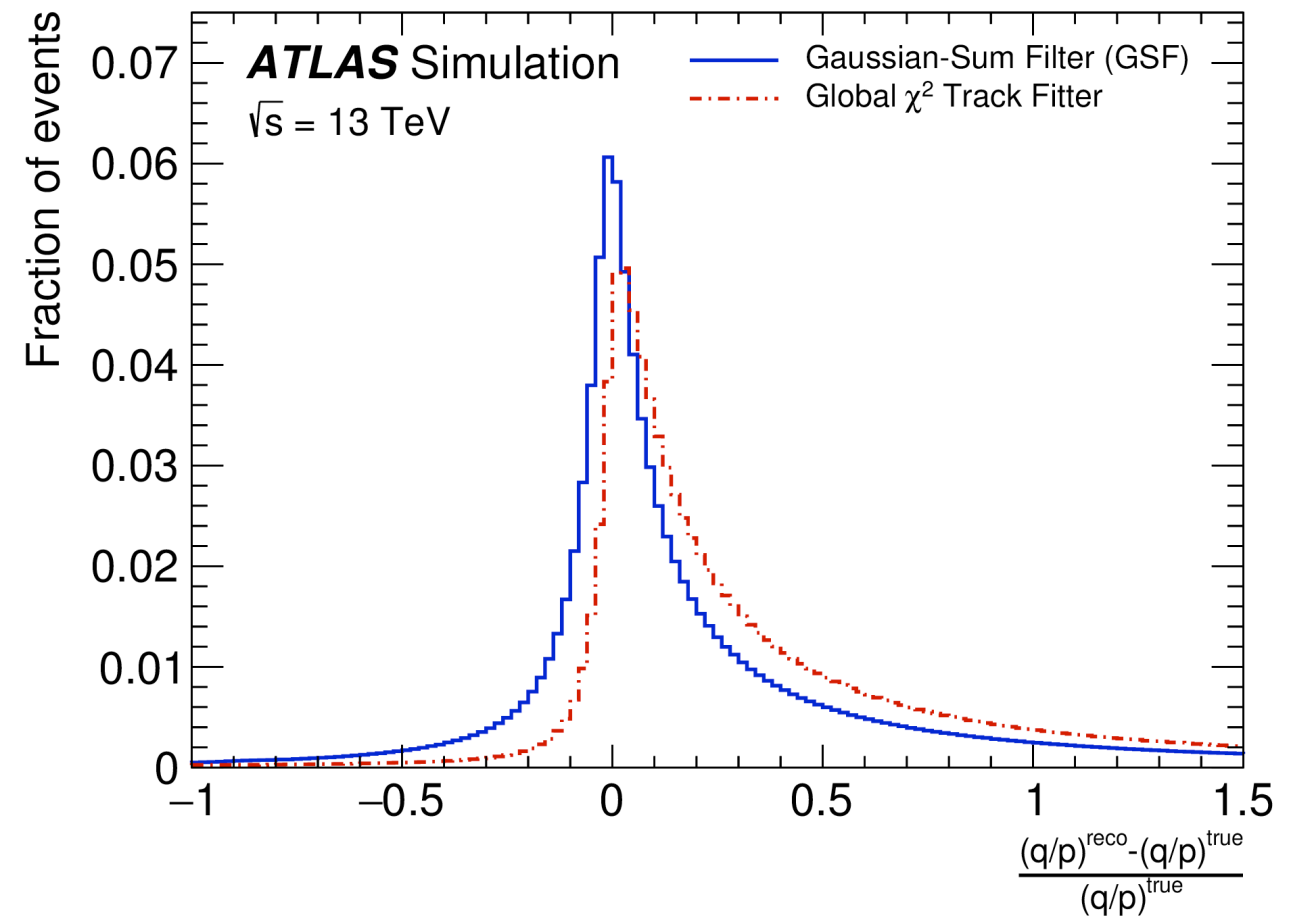
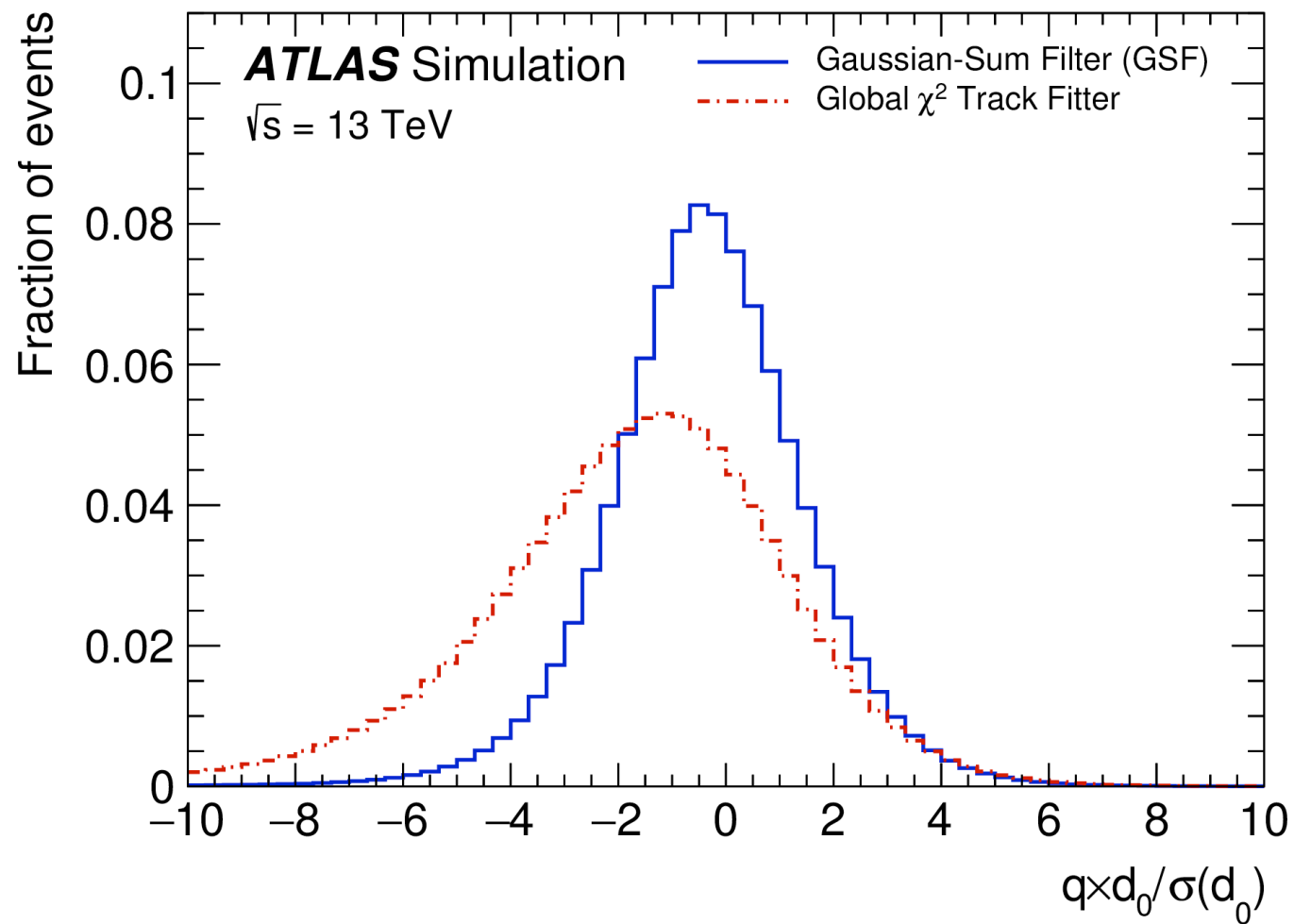
For a charged particle this is not the  $\phi$  at its vertex at it “bends”

For a photon converting depends on if we have captured the energy of both legs.



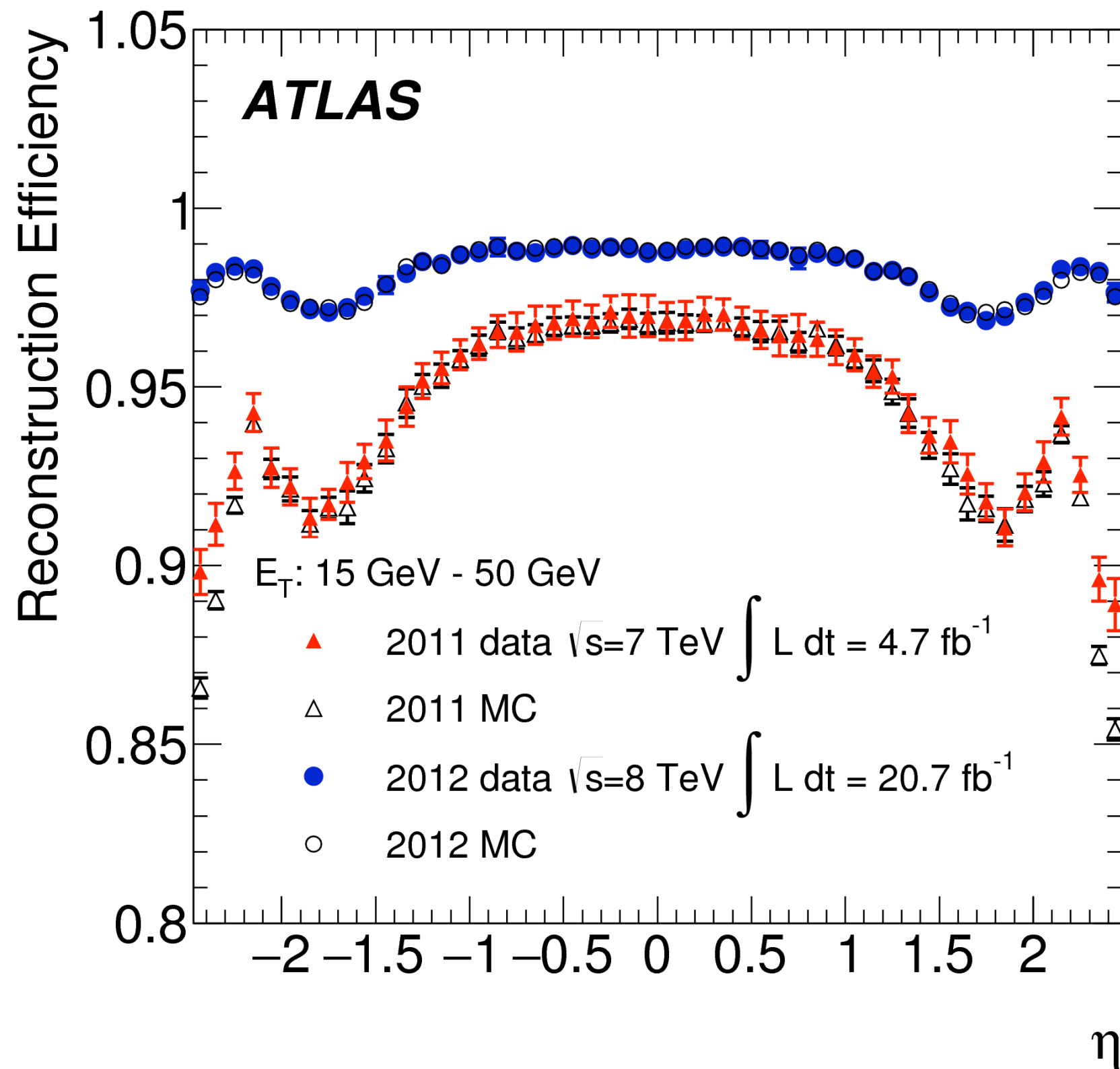
# e/ $\gamma$ specific tracking

This is basically the so called GSF (Gaussian Sum Filter) in ATLAS since 2011 (CMS much earlier)



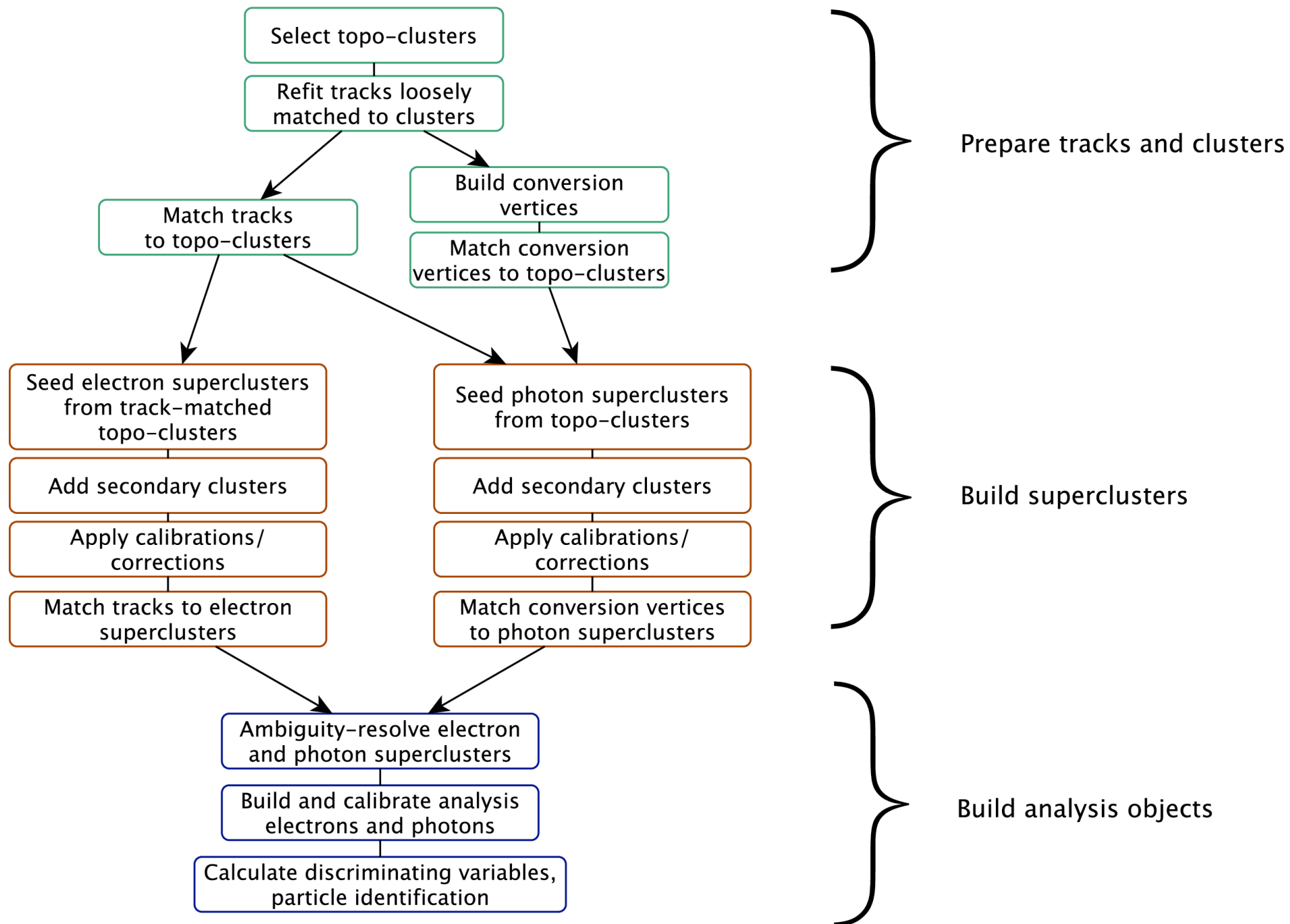
# $e/\gamma$ specific tracking

This is basically GSF (Gaussian Sum Filter) in ATLAS since 2012

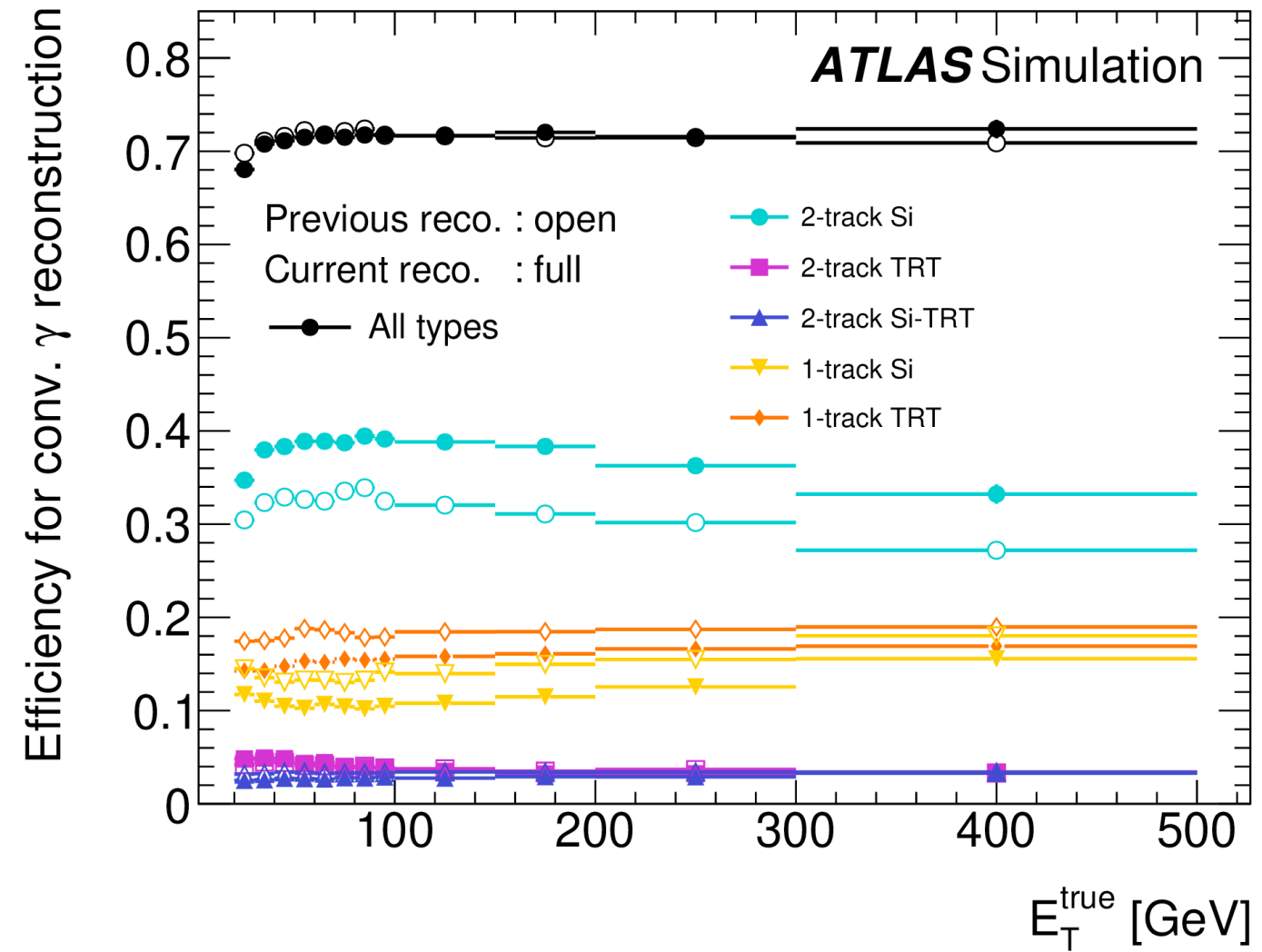
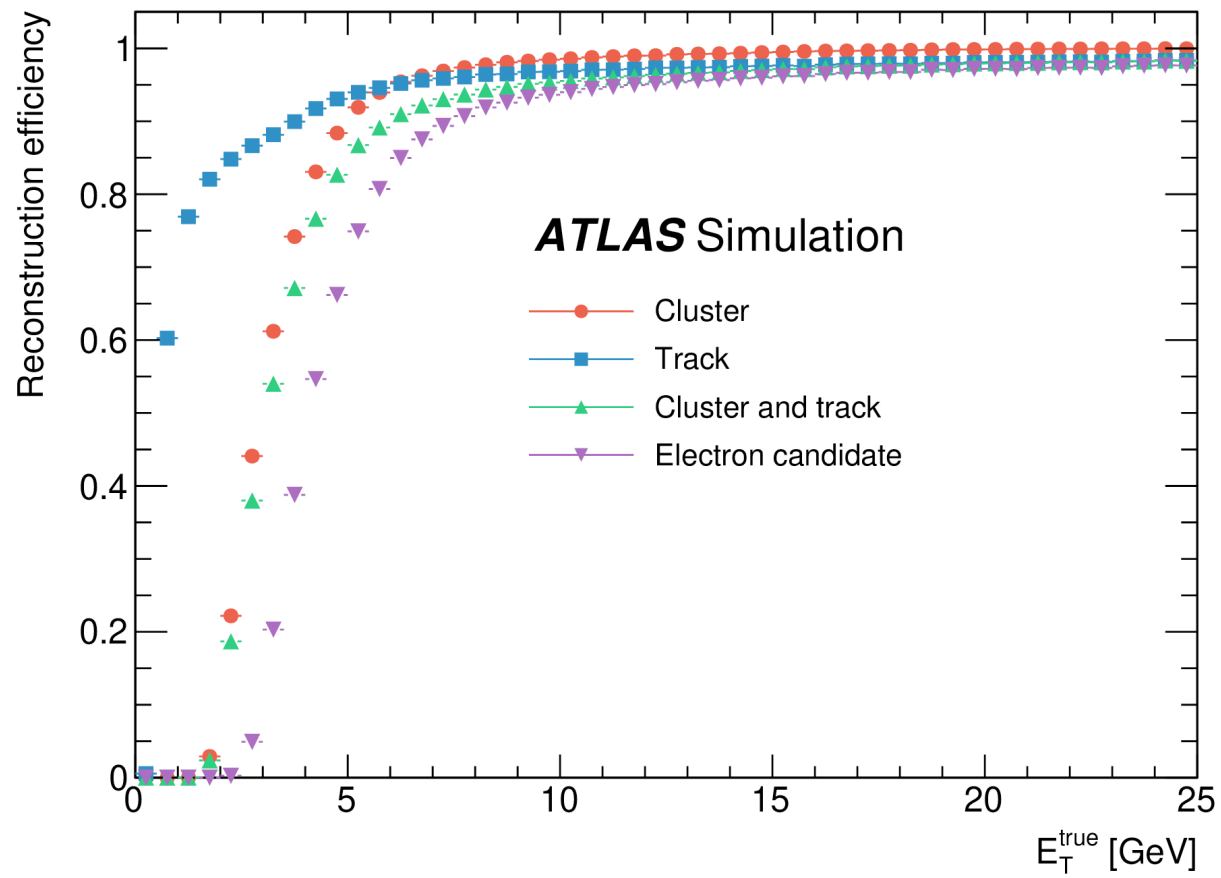




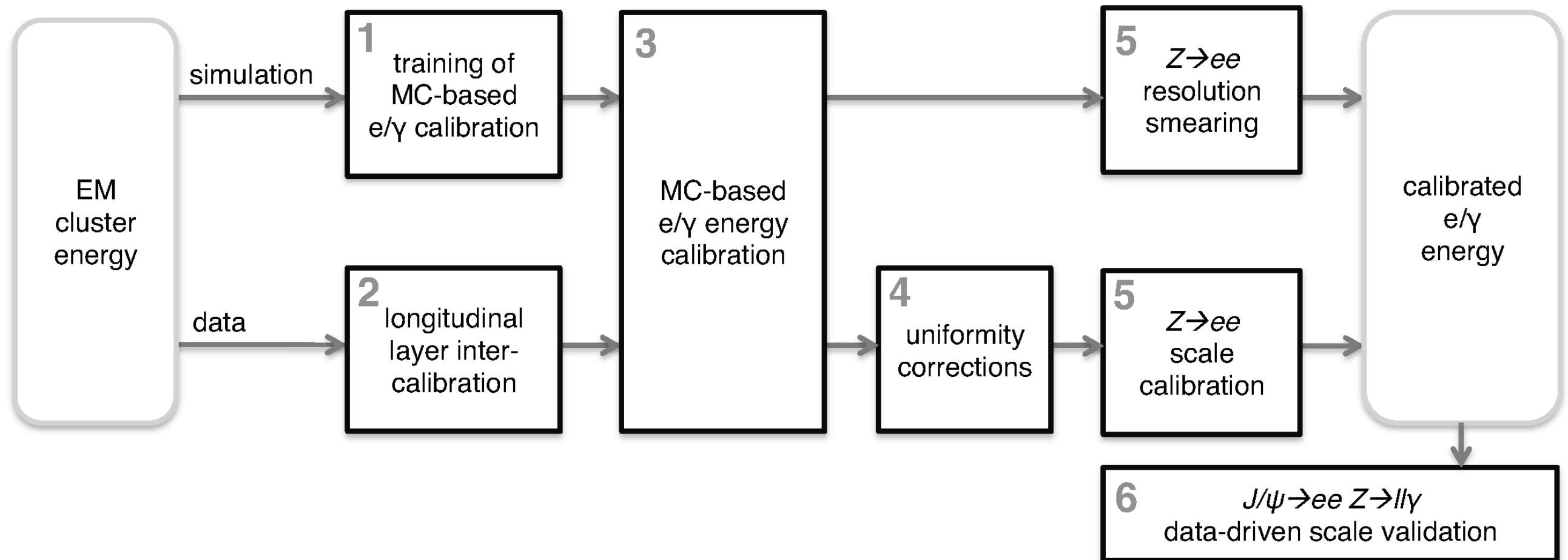
# $e/\gamma$ “the sausage machine”



# e/ $\gamma$ reconstruction



# e/γ calibration





# e/ $\gamma$ calibration

The different steps performed in the procedure to calibrate the energy response of electrons and photons from the energy of a cluster of cells in the EM calorimeter are the following:

- The estimation of the energy of the electron or photon from the energy deposits in the calorimeter: The properties of the shower development are used to optimize the energy resolution and to minimize the impact of material in front of the calorimeter. The multivariate regression algorithm used for this estimation is trained on samples of simulated events. The same algorithm is applied to data and simulation. This step relies on an accurate description of the material in front of the calorimeter in the simulation.
- The adjustment of the relative energy scales of the different layers of the EM calorimeter: This adjustment is based on studies of muon energy deposits and electron showers. It is applied as a correction to the data before the estimation of the energy of the electron or photon. This step is required for the correct extrapolation of the energy calibration to the full energy range of electrons and photons.
- The correction for residual local non-uniformities in the calorimeter response affecting the data: This includes geometric effects at the boundaries between calorimeter modules and improvements of the corrections for non-nominal HV settings in some regions of the calorimeter. This is studied using the ratio of the measured calorimeter energy to the track momentum for electrons and positrons from Z boson decays.

# e/γ calibration

- The adjustment of the overall energy scale in the data: This is done using a large sample of  $Z$  boson decays to electron–positron pairs. At the same time, a correction to account for the difference in energy resolution between data and simulation is derived, and applied to the simulation. These correction factors are assumed to be universal for electrons and photons.
- Checks of the results comparing data and simulation with independent samples:  $J/\psi \rightarrow ee$  decays probe the energy response for low-energy electrons. Radiative  $Z$  boson decays are used to check the energy response for photons.

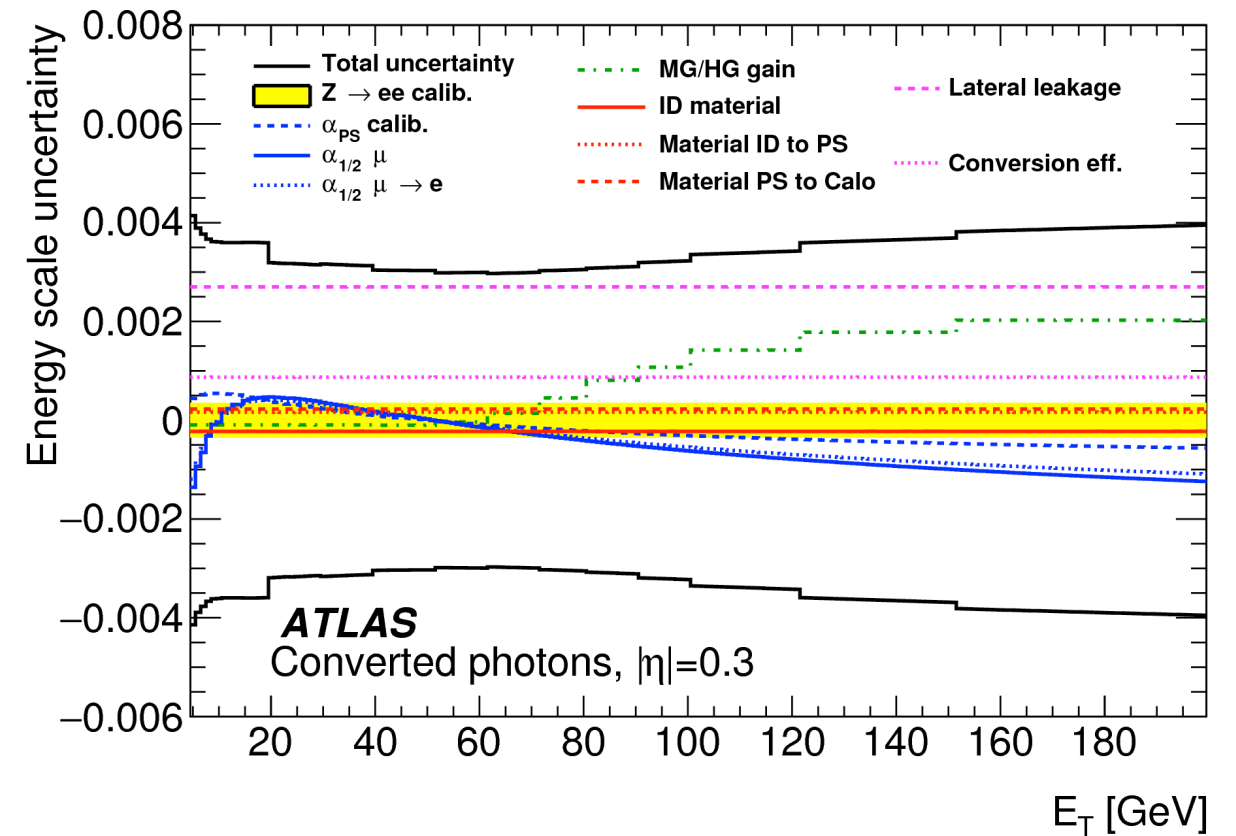
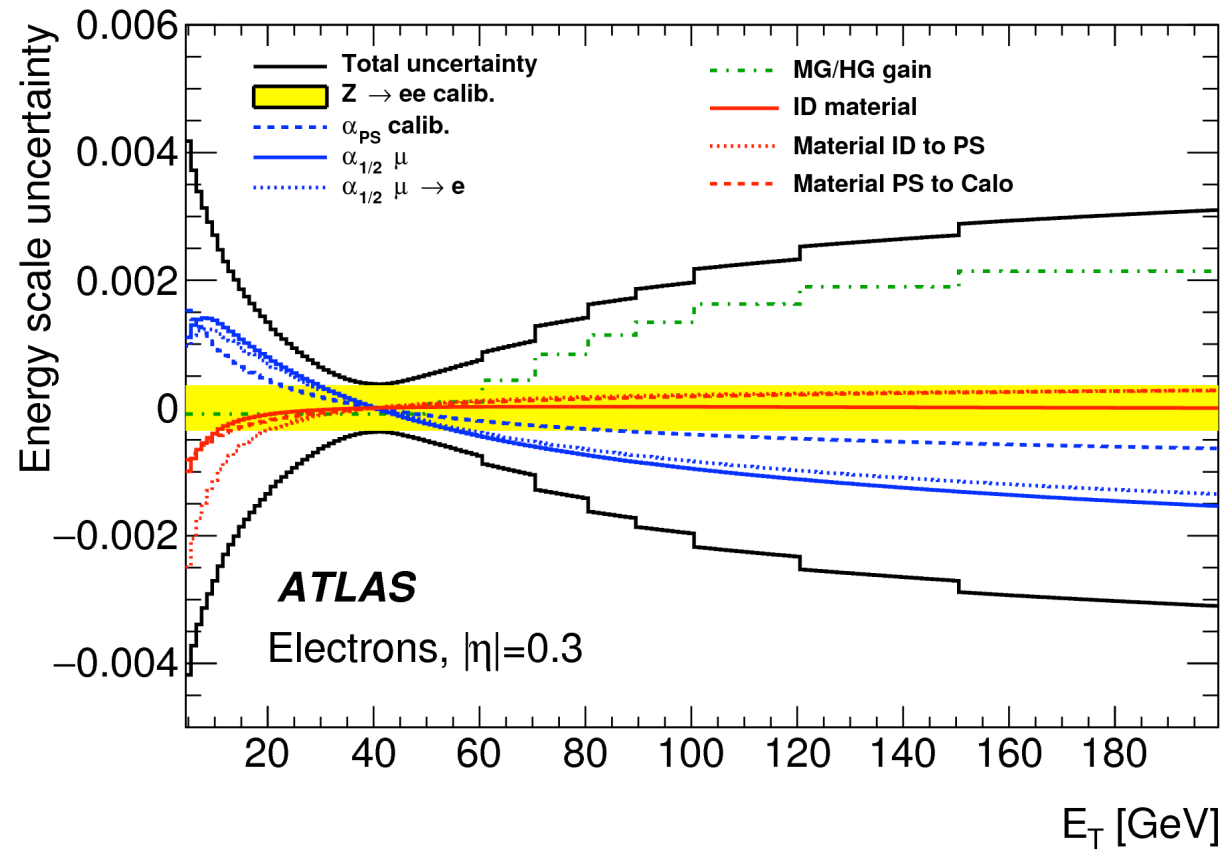
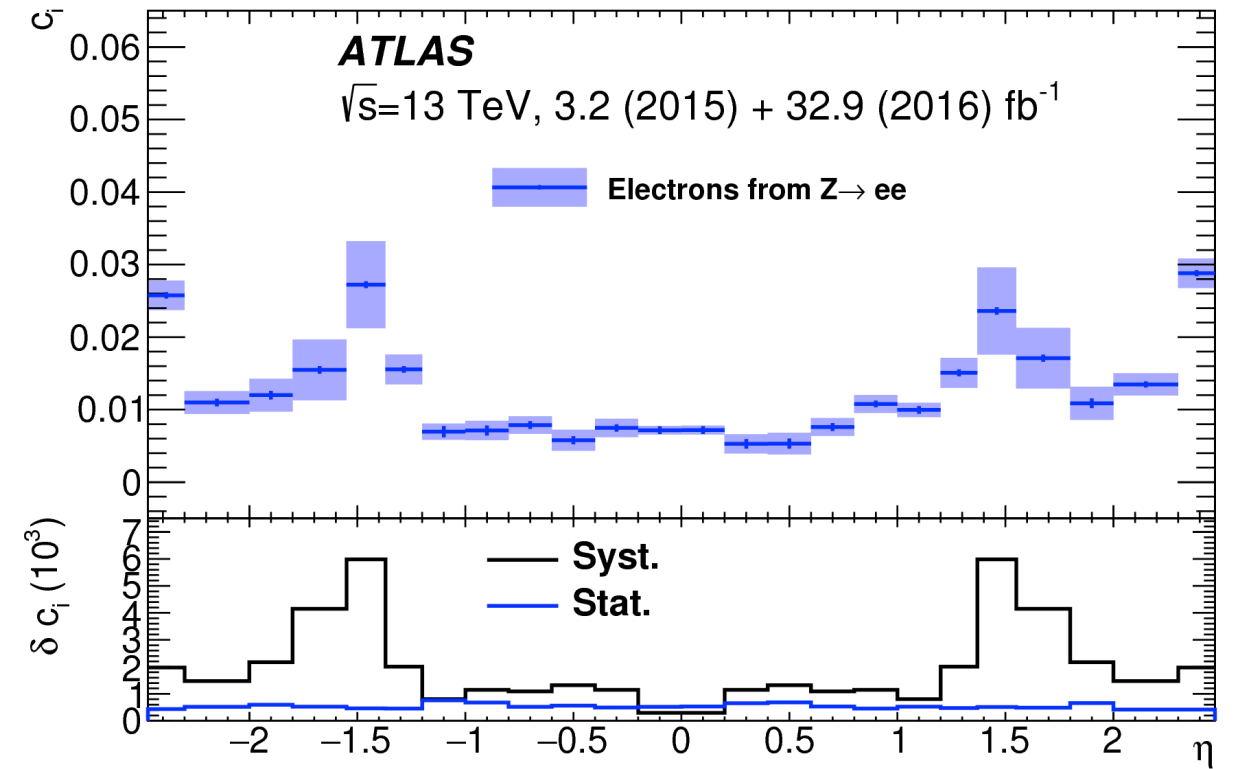
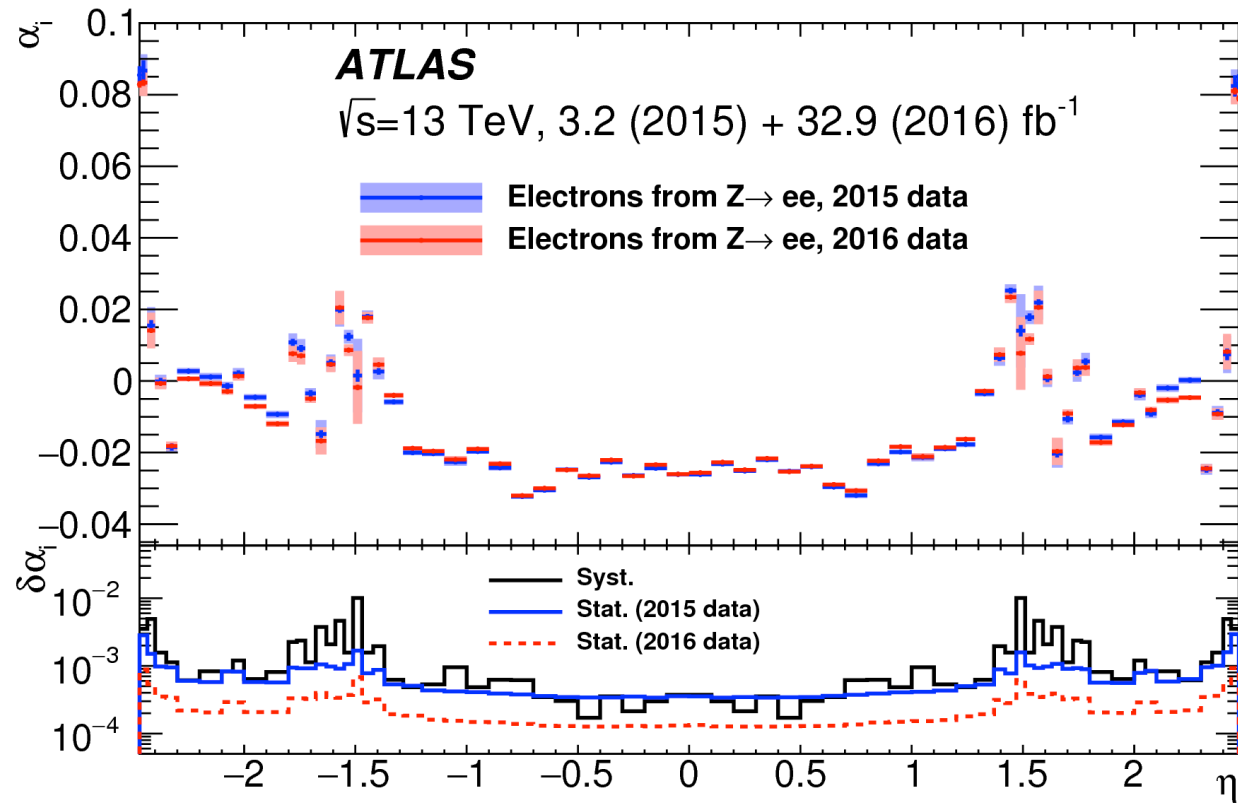
The difference in energy scale between data and MC simulation, after all the corrections described in Section 6 have been applied to the data, is defined as  $\alpha_i$ , where  $i$  corresponds to different regions in  $\eta$ . Similarly the difference in energy resolution is assumed to be an additional constant term in the energy resolution,  $c_i$ , depending on  $\eta$ :

$$E^{\text{data}} = E^{\text{MC}} (1 + \alpha_i), \quad \left( \frac{\sigma_E}{E} \right)^{\text{data}} = \left( \frac{\sigma_E}{E} \right)^{\text{MC}} \oplus c_i,$$

where the symbol  $\oplus$  denotes a sum in quadrature.



# e/γ calibration





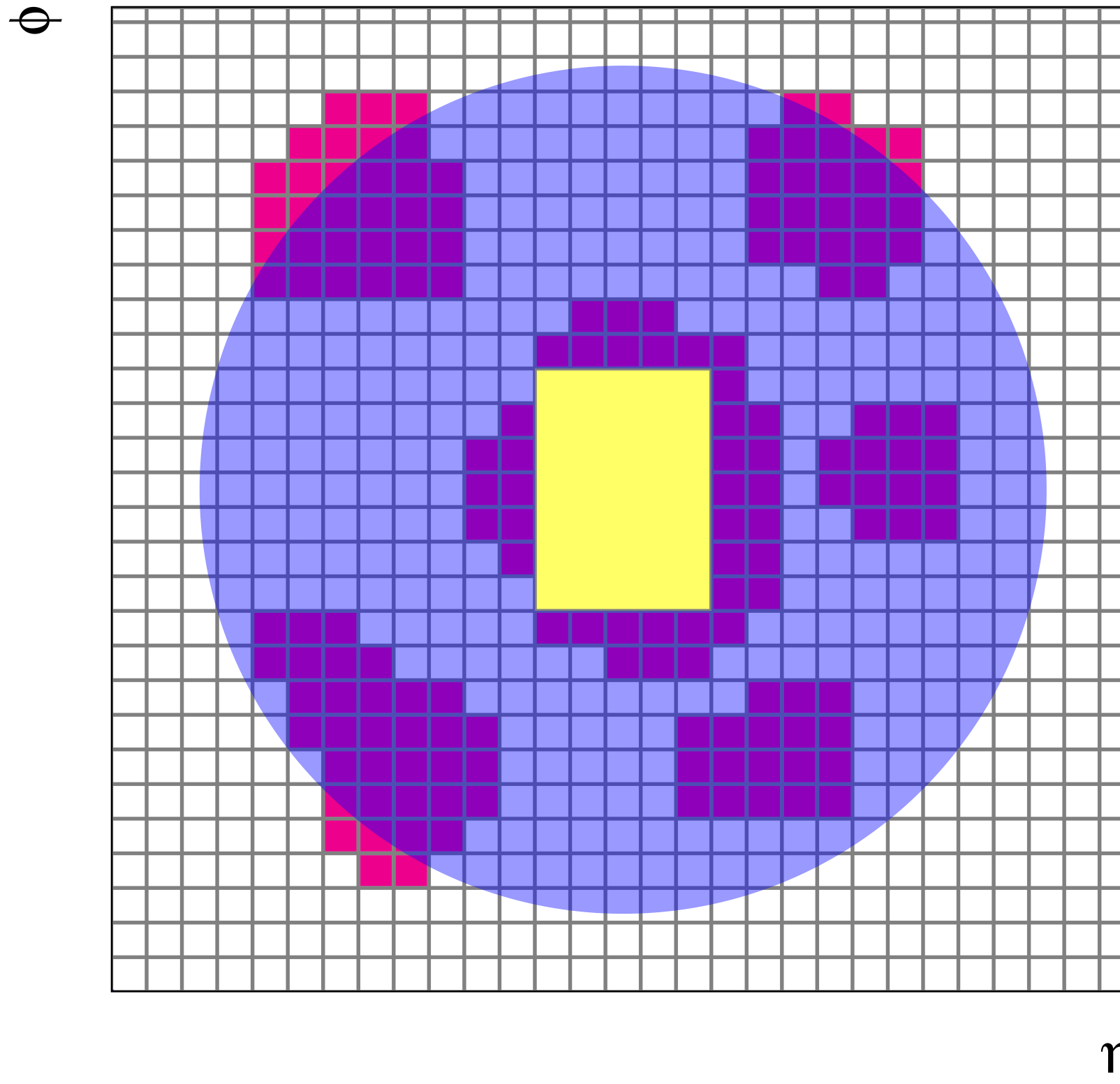
# e/γ identification

In the context of the discussion one thing to note is that we still deal with “rectangular” shapes.

Category	Description	Name	Usage
Hadronic leakage	Ratio of $E_T$ in the first layer of the hadronic calorimeter to $E_T$ of the EM cluster (used over the ranges $ \eta  < 0.8$ and $ \eta  > 1.37$ )	$R_{\text{had}_1}$	$e/\gamma$
	Ratio of $E_T$ in the hadronic calorimeter to $E_T$ of the EM cluster (used over the range $0.8 <  \eta  < 1.37$ )	$R_{\text{had}}$	$e/\gamma$
EM third layer	Ratio of the energy in the third layer to the total energy in the EM calorimeter	$f_3$	$e$
EM second layer	Ratio of the sum of the energies of the cells contained in a $3 \times 7 \eta \times \phi$ rectangle (measured in cell units) to the sum of the cell energies in a $7 \times 7$ rectangle, both centred around the most energetic cell	$R_\eta$	$e/\gamma$
	Lateral shower width, $\sqrt{(\sum E_i \eta_i^2)/(\sum E_i) - ((\sum E_i \eta_i)/(\sum E_i))^2}$ , where $E_i$ is the energy and $\eta_i$ is the pseudorapidity of cell $i$ and the sum is calculated within a window of $3 \times 5$ cells	$w_{\eta_2}$	$e/\gamma$
	Ratio of the sum of the energies of the cells contained in a $3 \times 3 \eta \times \phi$ rectangle (measured in cell units) to the sum of the cell energies in a $3 \times 7$ rectangle, both centred around the most energetic cell	$R_\phi$	$e/\gamma$
EM first layer	Total lateral shower width, $\sqrt{(\sum E_i (i - i_{\text{max}})^2)/(\sum E_i)}$ , where $i$ runs over all cells in a window of $\Delta\eta \approx 0.0625$ and $i_{\text{max}}$ is the index of the highest-energy cell	$w_{s \text{ tot}}$	$e/\gamma$
	Lateral shower width, $\sqrt{(\sum E_i (i - i_{\text{max}})^2)/(\sum E_i)}$ , where $i$ runs over all cells in a window of 3 cells around the highest-energy cell	$w_{s 3}$	$\gamma$
	Energy fraction outside core of three central cells, within seven cells	$f_{\text{side}}$	$\gamma$
	Difference between the energy of the cell associated with the second maximum, and the energy reconstructed in the cell with the smallest value found between the first and second maxima	$\Delta E_s$	$\gamma$
	Ratio of the energy difference between the maximum energy deposit and the energy deposit in a secondary maximum in the cluster to the sum of these energies	$E_{\text{ratio}}$	$e/\gamma$
	Ratio of the energy measured in the first layer of the electromagnetic calorimeter to the total energy of the EM cluster	$f_1$	$e/\gamma$
Track conditions	Number of hits in the innermost pixel layer	$n_{\text{innermost}}$	$e$
	Number of hits in the pixel detector	$n_{\text{Pixel}}$	$e$
	Total number of hits in the pixel and SCT detectors	$n_{\text{Si}}$	$e$
	Transverse impact parameter relative to the beam-line	$d_0$	$e$
	Significance of transverse impact parameter defined as the ratio of $d_0$ to its uncertainty	$ d_0/\sigma(d_0) $	$e$
	Momentum lost by the track between the perigee and the last measurement point divided by the momentum at perigee	$\Delta p/p$	$e$
	Likelihood probability based on transition radiation in the TRT	eProbabilityHT	$e$
Track-cluster matching	$\Delta\eta$ between the cluster position in the first layer of the EM calorimeter and the extrapolated track	$\Delta\eta_1$	$e$
	$\Delta\phi$ between the cluster position in the second layer of the EM calorimeter and the momentum-rescaled track, extrapolated from the perigee, times the charge $q$	$\Delta\phi_{\text{res}}$	$e$
	Ratio of the cluster energy to the measured track momentum	$E/p$	$e$

# e/ $\gamma$ identification

The first time we go to an explicit cone is later on in the isolation



# FSR recovery last minute

Final-state radiation (FSR) photons are searched for in all events following the procedure described in Ref. [13]. FSR candidates are defined as collinear if their angular separation from the nearest lepton of the quadruplet satisfies  $\Delta R < 0.15$ , and non-collinear otherwise. Collinear FSR candidates are considered only for muons from the leading dilepton, while non-collinear FSR candidates are considered for both muons and electrons from either the leading or the subleading dilepton. Only one FSR candidate is included in the quadruplet, with preference given to collinear FSR and to the candidate with the highest  $p_T$ . FSR photons are found in 4% of the events and their energy is included in the mass computation, improving the  $m_{4\ell}$  resolution by about 1%.

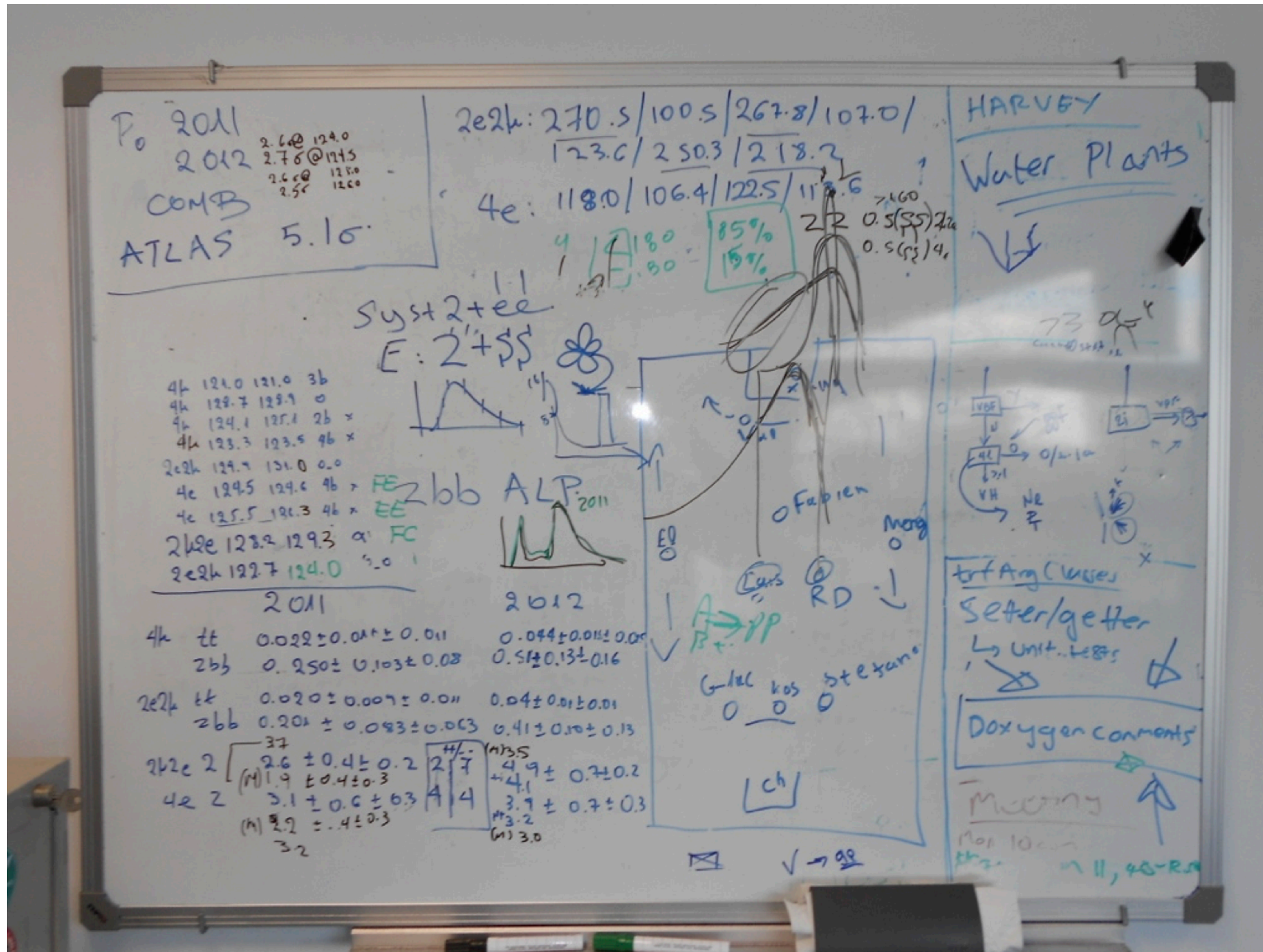
# Discussion ?

The e/ $\gamma$  reconstruction is geared towards dealing with material effects

- Special track fitter to account for brem.
- “Rectangular” fixed size/dynamic clusters “elongated” in  $\phi$  trying to collect as much as energy as possible.
- Still relative compact “size”
- In the calorimeter cluster level we do not differentiate between a “brem” and FSR photon.
- The energy collected in the “accordion” goes through a series of calibration steps. The last one is currently a BDT corrects for upstream and out of cluster etc losses.
- Perhaps important aside we employ a lot “single” particles samples in MC and we spent a lot of time on the material interactions side.
- Z data/MC enter later on in the chain .



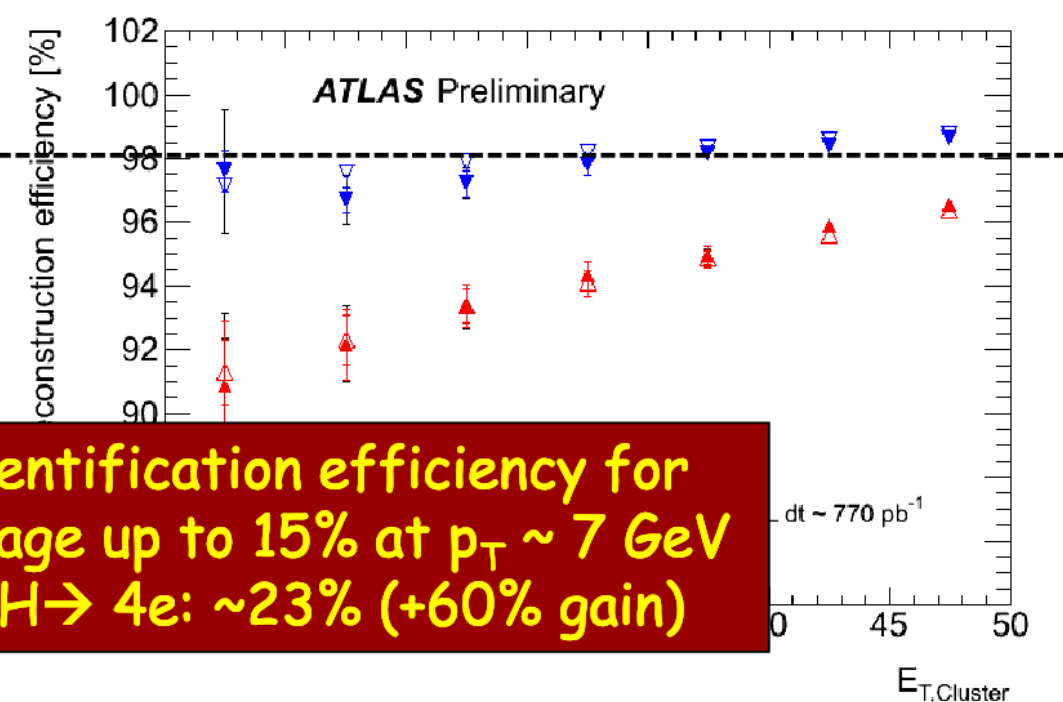
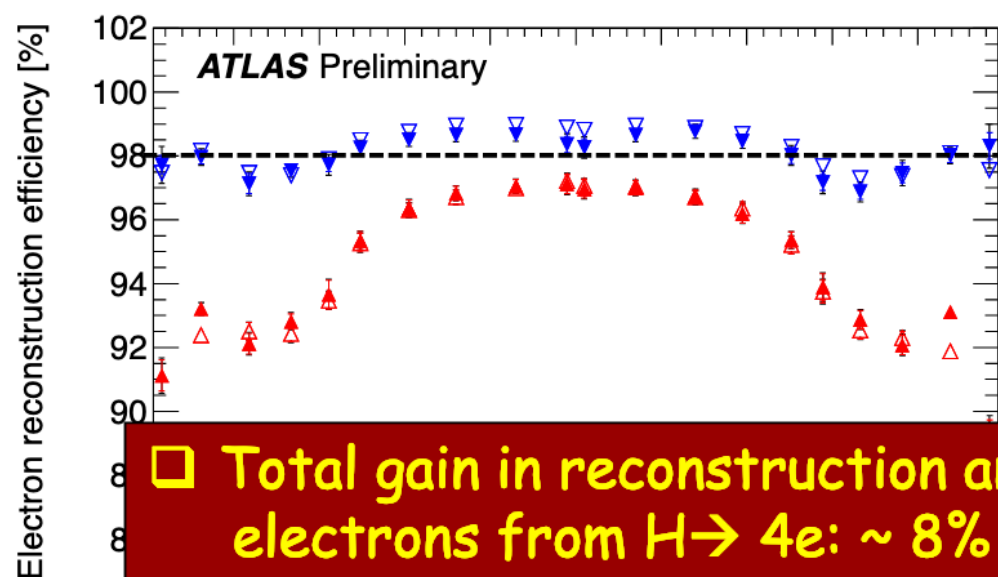
# Backup



# And more Performance

High efficiency for low- $p_T$  electrons (affected by material) crucial for  $H \rightarrow 4e, 2\mu 2e$

Improved track reconstruction and fitting to recover  $e^\pm$  undergoing hard Brem  
 $\rightarrow$  achieved  $\sim 98\%$  reconstruction efficiency, flatter vs  $\eta$  and  $E_T$



- Total gain in reconstruction and identification efficiency for electrons from  $H \rightarrow 4e$ :  $\sim 8\%$  average up to  $15\%$  at  $p_T \sim 7 \text{ GeV}$
- Total acceptance  $\times$  efficiency for  $H \rightarrow 4e$ :  $\sim 23\%$  (+60% gain)

Re-optimized  $e^\pm$  identification using pile-up robust variables (e.g. Transition Radiation, calorimeter strips)  $\rightarrow$  achieved  $\sim 95\%$  identification efficiency,  $\sim$  flat vs pile-up; higher rejections of fakes

Results are from  $Z \rightarrow ee$  data and MC tag-and-probe

